CHEMMEDCHEM

DOI: 10.1002/cmdc.200900459

Design, Synthesis and Biological Evaluation of Carboxy Analogues of Arginine Methyltransferase Inhibitor 1 (AMI-1)

Sabrina Castellano,[a] Ciro Milite,[a] Rino Ragno,[b] Silvia Simeoni,[b] Antonello Mai,[b] Vittorio Limongelli,[c] Ettore Novellino,[c] Ingo Bauer,[d] Gerald Brosch,[d] Astrid Spannhoff,[e] Donghang Cheng,[e] Mark T. Bedford,*[e] and Gianluca Sbardella*[a]

Dedicated to Professor Marino Artico on the occasion of his 75th birthday.

Here we report the synthesis of a number of compounds structurally related to arginine methyltransferase inhibitor 1 (AMI-1). The structural alterations that we made included: 1) the substitution of the sulfonic groups with the bioisosteric carboxylic groups; 2) the replacement of the ureidic function with a bisamidic moiety; 3) the introduction of a N-containing basic moiety; and 4) the positional isomerization of the aminohydroxynaphthoic moiety. We have assessed the biological activity of these compounds against a panel of arginine methyltransferases (fungal RmtA, hPRMT1, hCARM1, hPRMT3, hPRMT6) and a lysine methyltransferase (SET7/9) using histone and nonhistone proteins as substrates. Molecular modeling studies for a deep binding-mode analysis of test compounds were also performed. The bis-carboxylic acid derivatives **1b** and **7b** emerged as the most effective PRMT inhibitors, both in vitro and in vivo, being comparable or even better than the reference compound (AMI-1) and practically inactive against the lysine methyltransferase SET7/9.

Introduction

Besides allowing the cell to expand its repertoire over the constraints imposed by the twenty encoded amino acids, post-translational modifications of proteins play pivotal roles in chromatin-templated nuclear events, such as transcription and DNA damage repair.[1–3] The methylation of arginine residues is a prevalent post-translational modification, found on both nuclear and cytoplasmic proteins, catalyzed by the protein arginine *N*-methyltransferase (PRMT) family of enzymes. Arginine-methylated proteins are involved in a number of different cellular processes, including transcriptional regulation, RNA metabolism and DNA damage repair.[4–7] Most PRMTs methylate glycine- and arginine-rich patches (GAR motifs) within their substrates, using *S*-adenosylmethionine (SAM) as the methyl donor.[8,9] The complexity of the methylarginine marker is enhanced by the ability of this residue to be methylated in three different ways on the guanidino group: monomethylated (MMA), symmetrically dimethylated (*s*DMA) and asymmetrically dimethylated (*a*DMA), each of which has potentially different functional consequences.[4]

To date, ten mammalian PRMTs have been identified; they are classified as type I, type II, type III or type IV enzymes.[9] Types I, II and III methylate the terminal (or ω) guanidino nitrogen atoms; type I PRMTs (PRMT1, 3, 4, 6 and 8) catalyze the production of *a*DMA, whereas type II PRMTs (PRMT5, PRMT7 and FBXO11) catalyze the formation of *s*DMA. PRMT7, a type III enzyme, catalyzes the formation of MMA on certain substrates, but does catalyze the formation of *s*DMA catalysis. A type IV enzyme that catalyzes the monomethylation of the internal (or δ) guanidino nitrogen atom has been described in yeast.[9] An increasing amount of evidence shows the involvement of PRMTs in a wide variety of cellular processes, including nuclear hormone receptor-mediated signaling, protein–protein interactions, protein trafficking, *m*RNA splicing and processing, and transcriptional regulation.[4,6,9,10] In particular, PRMT1 plays a key role in the shuttling of heterogeneous nuclear ribonucleoproteins (*hn*RNPs) between the cytoplasm and the nucleus[9,11] and is a transcriptional coactivator for multiple nuclear receptor family members (e.g., the androgen and estrogen receptors),[12–14] being recruited to promoters by a number of differ-

[a] *Dr. S. Castellano, Dr. C. Milite, Prof. G. Sbardella*
Dipartimento di Scienze Farmaceutiche, Università degli Studi di Salerno
Via Ponte Don Melillo, 84084 Fisciano SA (Italy)
Fax: (+39) 089-96-9602
E-mail: gsbardella@unisa.it

[b] *Dr. R. Ragno, Dr. S. Simeoni, Prof. A. Mai*
Dipartimento di Chimica e Tecnologie del Farmaco, Sapienza Università di Roma, P. le A. Moro 5, 00185 Roma (Italy)

[c] *Dr. V. Limongelli, Prof. E. Novellino*
Dipartimento di Chimica Farmaceutica e Tossicologica, Università di Napoli "Federico II", Via D. Montesano 49, 80131 Napoli (Italy)

[d] *Dr. I. Bauer, Prof. G. Brosch*
Division of Molecular Biology, Biocenter-Innsbruck Medical University
Fritz-Preglstrasse 3, 6020 Innsbruck (Austria)

[e] *Dr. A. Spannhoff, Dr. D. Cheng, Prof. M. T. Bedford*
University of Texas M.D. Anderson Cancer Center, Science Park-Research Division, Smithville, Texas 78957 (USA)
Fax: (+1) 512-237-2475
E-mail: mtbedford@mdanderson.org

Supporting information for this article is available on the WWW under http://dx.doi.org/10.1002/cmdc.200900459.

ent transcription factors.[4,9] Dysregulation of nuclear receptor signaling is a hallmark of hormone-dependent cancers, such as, breast cancer.[15–18] In addition to this, PRMT1 has recently emerged as a potential new target for the development of a novel therapeutic for heart disease,[19–26] as it appears to be responsible for generating the majority of *a*DMA and it is overexpressed in the hearts of patients with coronary heart disease.[27]

Similarly, CARM1, sometimes referred to as PRMT4, has been shown to methylate many coactivators, including p300/CBP and AIB1 (amplified in breast cancer-1),[4] as well as proteins involved in splicing[28] and RNA-binding proteins,[3,29,30] thus playing a crucial role in modulating gene expression at multiple critical levels.[9] Recently it was reported that CARM1 is upregulated during the progression of prostate cancer,[20] and that CARM1 and PRMT1 synergistically coactivate NF-κB-dependent gene expression.[31] Therefore, convincing evidence supports the hypothesis that targeting PRMTs would be a viable approach in anticancer therapy.

Despite extensive research aimed at better understand the role of PRMTs in physiological and pathological pathways,[9,12–24,26] elucidating the structure[32–34] of these enzymes, and gaining insights into the mechanism of methyl transfer,[35] there have been only a few publications to date describing small-molecule chemical modulators of the PRMTs (Figure 1).[36–46]

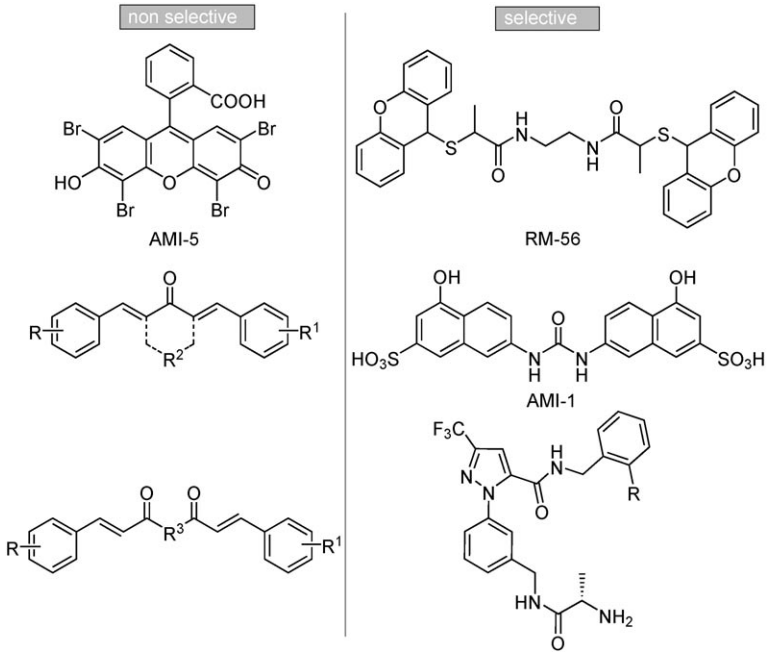

Figure 1. Small molecule inhibitors of PRMTs.

Among them, 7,7′-carbonylbis(azanediyl)bis(4-hydroxynaphthalene-2-sulfonic acid) (AMI-1, Figure 1) was identified in 2004 through a random screening effort by Bedford and co-workers as a compound able to inhibit arginine, but not lysine methylation, being noncompetitive with *S*-adenosylmethionine (SAM) binding.[36] To date, AMI-1 is the most active nonpeptidic[47] inhibitor reported to be selective against PRMT1; other compounds are from 1.5- to approximately 45-fold less active.[41,42]

Prompted by our interest in the discovery of small-molecule modulators of epigenetic targets,[37,38,40,48–55] we focused our attention on AMI compounds and noticed the occurrence of dye-like scaffolds as a common feature.[40] Therefore, we carried out molecular modeling studies and described the binding mode analysis of a focused library of small molecules into the catalytic domain of both *h*PRMT1 and its fungal homologue RmtA, validated by us as a preliminary screening tool for arginine methyltransferase inhibitors.[40] We also performed enzymatic assays on recombinant RmtA and PRMT1 proteins using SAM and histones as substrates, and obtained a good agreement between biological and computational results. The major outcomes of the docking and binding mode analysis (the reliability of which was then confirmed by structure-based three-dimensional QSAR models[56]) were the positioning of AMI-1 between the SAM and arginine binding sites without fully occupying them, whereas the nonarginine-selective derivative AMI-5 (Figure 1) was positioned in the SAM binding site.[40] This is consistent with previously reported kinetics experiments.[36] Moreover, these analyses hinted that two regions in the RmtA catalytic site, the pocket formed by Ile 12, His 13, Met 16, and Thr 49 (dark gray area in Figure 2)[57] and the SAM methioninic portion binding site delimited by Arg 22, Asp 44, Gly 46, Cys 47, Ile 51, Leu 52 and Glu 112 (light gray area in Figure 2), should be taken into account when designing novel inhibitors.[40]

However, before undertaking the exploration of the two aforementioned additional pockets, we realized that AMI-1 should be optimized as it is likely to have low bioavailability and would probably not penetrate the blood–brain barrier due to the bisanionic structure. Moreover, it is related to suramin-type sulfonated ureas, reported to give pleiotropic interactions with many proteins.[58,59]

Therefore, we designed a number of derivatives characterized by the substitution of the sulfonic groups with the bioisosteric carboxylic groups, the replacement of the ureidic function with a bisamidic moiety, the introduction of a N-containing basic moiety or the positional isomerization of the aminohydroxynaphthoic moiety (Figure 3).

Here, we describe in detail the synthesis of compounds **1**–**9** and their biological evaluation against a panel of PRMTs (fungal RmtA, *h*PRMT1, *h*CARM1, *h*PRMT3, *h*PRMT6), as well as against a lysine methyltransferase, SET7/9.

Results and Discussion

Chemistry

The key step in the synthesis of derivatives **1**–**6** (Scheme 1) was the preparation of **12a**. Following a highly efficient procedure recently described by us,[60] we used a Wittig reaction be-

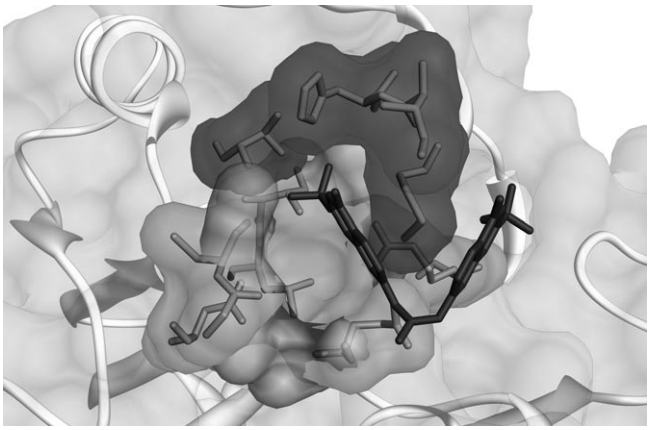

Figure 2. The two additional binding pockets in the RmtA catalytic site that emerged from three-dimensional QSAR studies. The area highlighted in light gray[57] is delimited by Arg 22, Asp 44, Gly 46, Cys 47, Ile 51, Leu 52 and Glu 112, whereas the area depicted in dark gray is formed by Ile 12, His 13, Met 16, and Thr 49. The binding mode of AMI-1 (stick representation, carbon atoms in gray) is also shown.

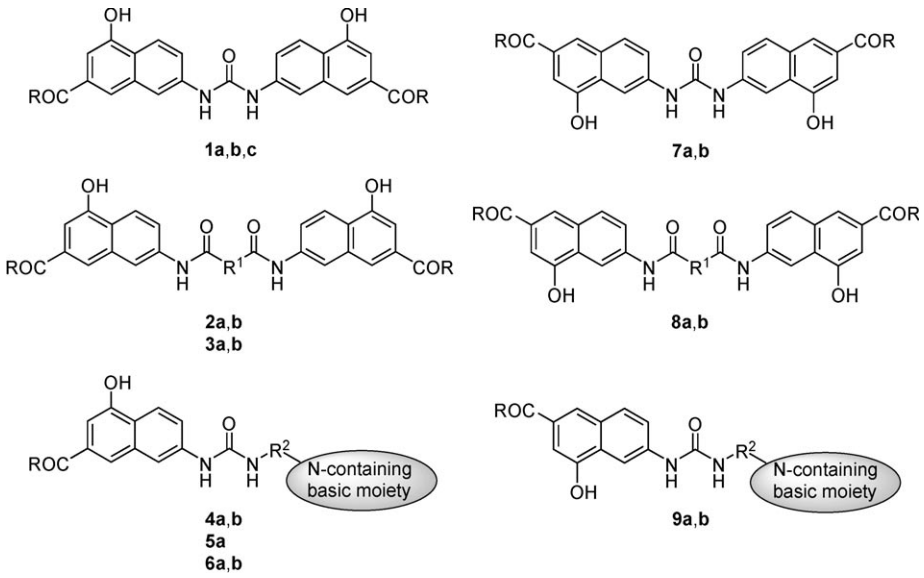

Figure 3. Novel AMI-1 analogues.

tween 3-nitrobenzaldehyde and carboxyphosphorane **10**[61] to regioselectively prepare the (*E*)-nitrophenylitaconate **11a**, which was selectively reduced with zinc dust in acetic acid to give the amino derivative **11b** (Scheme 1). Ring closure via microwave-assisted Friedel–Crafts acylation[60] followed by the hydrolysis of the crude product and subsequent esterification furnished a mixture of 5-amino- and 7-amino-substituted naphthoic esters from which **12a** was conveniently obtained by precipitating its 5-amino- isomer **12b** as an insoluble cobalt(II) complex salt.

The symmetrical ureidic derivative **1a** was directly obtained by reacting **12a** with diphenyl carbonate in refluxing chlorobenzene in the presence of DMAP. The following hydrolysis with aqueous sodium hydroxide and pyridine in tetrahydrofuran furnished the corresponding acid **1b** (Scheme 1), whereas the treatment of the ester **1a** with aqueous ammonia gave the bisamidic derivative **1c**. Conversely, the unsymmetrical ureidic derivatives were prepared by treating **12a** with trichloroacetylchloride in dichloromethane and reacting the resulting trichloroacetamide **14** with the appropriate amine to obtain compounds **4a**, **5a** and **6a**, the hydrolysis of which yielded acids **4b** and **6b**, respectively (Scheme 1).[62]

With regard to bisamidic derivatives, the reaction of **12a** with succinyl chloride in the presence of triethylamine yielded ester **3a**, which was hydrolyzed to the acid **3b** following the aforementioned protocol. The reaction of **12a** with malonyl chloride under these conditions failed and the malonyl diamide **2a** was obtained via a different route in two steps: one equivalent of compound **12a** was reacted with an excess of neat diethyl malonate by microwave irradiation, and then a second equivalent of the compound was added as a solution in *N*-methylpyrrolidone/toluene (1:10). Again, subsequent hydrolysis of **2a** gave the corresponding acid **2b**.

The absence of regioselectivity in the preparation of the 7-amino-4-hydroxy-2-naphthoic ester **12a**, which had to be separated from the 5-amino-substituted isomer **12b**,[60] hindered the assembly of a focused library based on this intermediate with which we intended to explore the two aforementioned pockets that emerged from computational studies (Figure 2). Therefore, we decided to synthesize derivatives **7a**,**b**, **8a**,**b** and **9a**,**b**, positional isomers of **1a**,**b**, **2a**,**b** and **4a**,**b**, respectively, and to evaluate their biological activities.

The Wittig reaction between 4-nitrobenzaldehyde and carboxyphosphorane **10**, followed by the microwave-assisted Friedel–Crafts-type ring closure, yielded only methyl 4-acetoxy-6-nitro-2-naphthoate **15**, which was promptly reduced to the key intermediate **16** by heterogeneous catalytic hydrogenation (Scheme 2).

The reaction of **16** with diphenyl carbonate in refluxing chlorobenzene followed by the hydrolysis of the acetoxy group with potassium carbonate gave the symmetrical ureidic derivative **7a**. The subsequent hydrolysis with aqueous sodium hydroxide and pyridine in tetrahydrofuran furnished the corresponding acid **7b** (Scheme 2). Conversely, the unsymmetrical ureidic derivatives were prepared by treating **16** with trichloroacetylchloride to give the corresponding trichloroacetamides **18**[63] and then reacting these with tryptamine to obtain the ester **9a**. The hydrolysis of the latter yielded the corresponding acid **9b** (Scheme 2). Finally, the two-step reaction under micro-

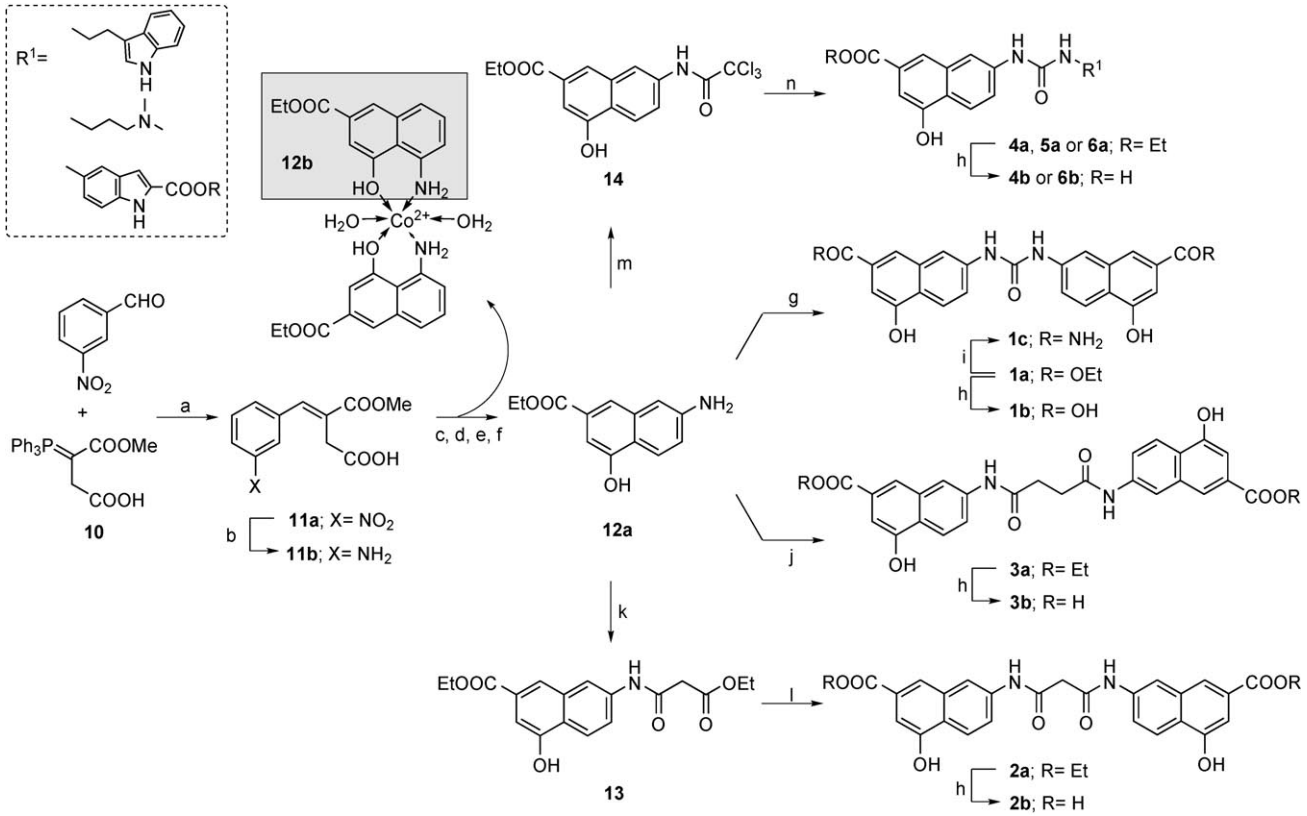

Scheme 1. *Reagents and conditions*: a) benzene, RT, 48 h; b) Zn, AcOH, RT, 24 h; c) NaOAc, Ac_2O, MW (300 W, 5 min); d) aq 8 N HCl, 5 h; e) EtOH, H_2SO_4, reflux, 24 h; f) $Co(OAc)_2{\cdot}4H_2O$, AcOH/NaOAc pH 5 buffer, CH_3OH; g) diphenylcarbonate, DMAP, chlorobenzene, reflux, 72 h; h) aq NaOH, pyridine, THF, RT; i) aq NH_3, RT, 12 h; j) succinyl chloride, Et_3N, acetone, RT, 4 h; k) diethyl malonate, MW (300 W, 30 min), neat; l) **12a**, toluene/NMP (10:1), MW (300 W, 3×30 min); m) $ClCOCCl_3$, CH_2Cl_2, RT, 4 h; n) R^1NH_2, K_2CO_3, DMF, 150 °C, 1 h, sealed tube.

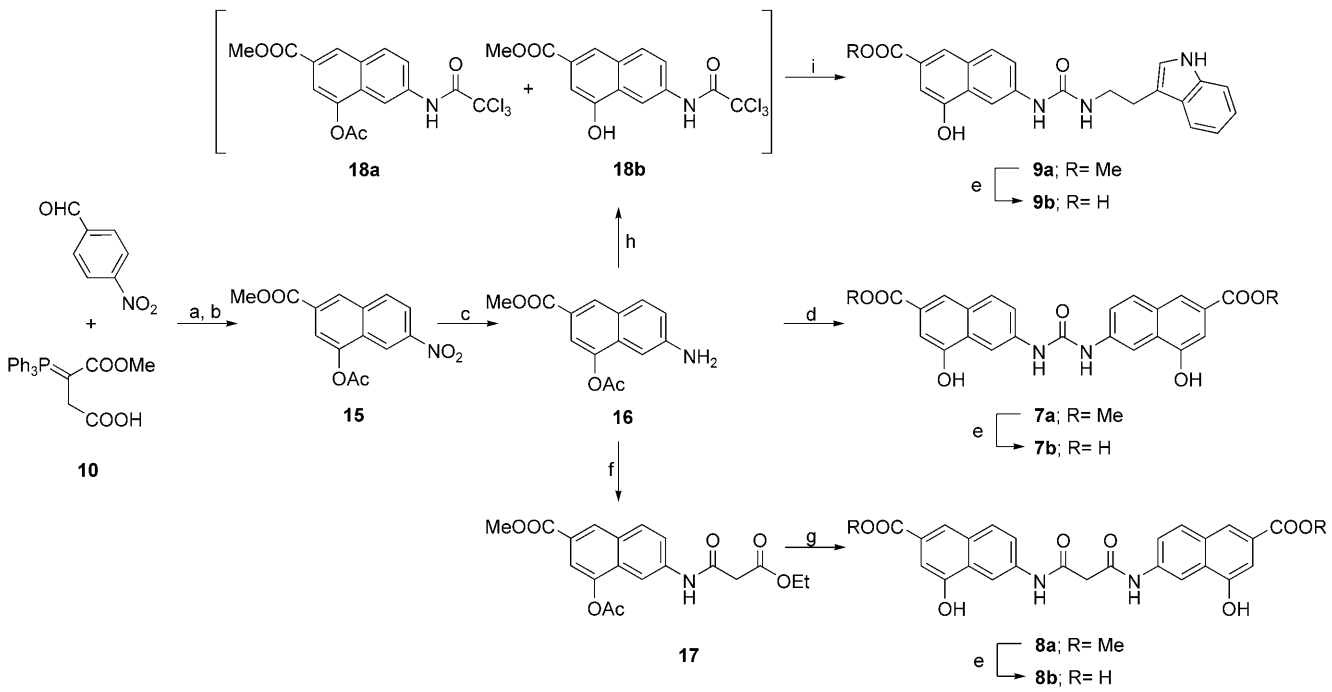

Scheme 2. *Reagents and conditions*: a) benzene, RT, 48 h; b) NaOAc, Ac_2O, MW (300 W, 5 min); c) H_2, Pd/C, EtOH, 2 h; d) 1) diphenylcarbonate, DMAP, chlorobenzene, reflux, 72 h; 2) K_2CO_3, EtOH, 70 °C, 2 h; e) aq NaOH, pyridine, THF, RT; f) diethyl malonate, MW (300 W, 30 min), neat; g) 1) **16**, toluene/NMP (10:1), MW (300 W, 3×30 min); 2) K_2CO_3, EtOH, 70 °C, 2 h; h) $ClCOCCl_3$, CH_2Cl_2, RT, 4 h; i) tryptamine, K_2CO_3, DMF, 150 °C, 1 h, sealed tube.

wave irradiation between **16** and diethyl malonate, followed by the hydrolysis of the acetoxy group with potassium carbonate, yielded the malonyl diamide **8a**. Again, subsequent hydrolysis of **8a** gave the corresponding acid **8b** (Scheme 2).

Biology

In accordance with our previous studies,[37,40] we first performed a preliminary screening of the activities of compounds **1**–**9** against *Aspergillus nidulans* RmtA, a fungal PRMT acting on histone H4 substrate and validated by us as a useful, predictive model for studying PRMT inhibition in mammals.[40] Then we tested the derivatives against human recombinant PRMT1 in vitro, using histone as well as nonhistone (the RNA-binding nuclear shuttling protein, Npl3) proteins as a substrate, to confirm their inhibitory activity and to observe the influence of substrates different from histones on the inhibitory activity. Subsequently, selected compounds were tested (50 μM) against a panel of human PRMTs (PRMT1, PRMT3, CARM1, and PRMT6), using histone H4 (for PRMT1), histone H3 (for CARM1 and PRMT6) or GAR (for PRMT3) motifs as substrates. Furthermore, to assess the selectivity of our compounds against lysine methyltransferases, we also tested our compounds against the HKMT SET7/9 using histone H3 as a substrate.

Inhibitory activities against RmtA and PRMT1

Compounds **1**–**9** were preliminarily tested against *Aspergillus nidulans* RmtA, a fungal PRMT with significant sequence similarity to human PRMT1 and specific for methylation at Arg 3 of histone H4,[64] and against *h*PRMT1, using core histones as substrate as previously described.[40,64] The inhibition (%) at a fixed dose (nearly 100 μM) were first determined (data not shown), and then the IC_{50} values for the active compounds were established (Table 1).

Moreover, the derivatives were also tested against *h*PRMT1, using the heterogeneous nuclear ribonucleoprotein (*hn*RNP) Npl3p, an in vivo substrate of HMT1 from *Saccharomyces cerevisiae*,[65] as a substrate. The inhibition (%) at fixed doses (10 and 50 μM) were determined (Table 2). AMI-1 was used as reference compound in both assays.

The first result that emerged from both assays was that the substitution of the AMI-1 sulfonic group with its carboxylic isoster gave only a slight decrease in inhibiting activity (cf. AMI-1 and **1b**, Tables 1 and 2). Conversely, the replacement of the carboxylic group with an ester or an amide function diminished the activity against PRMT1. There was no difference in the order of activity when histone or nonhistone proteins were used as the substrate (**1b** > **1c** > **1a**), however, a slightly different order resulted when compared to the results obtained against RmtA (**1b** > **1a** > **1c**).

The substitution of the ureidic group with bisamidic moieties was detrimental to the inhibitory potency of the resulting derivatives, with the decrease being proportional to the length of the aliphatic spacer (cf. inhibition (%) values of compounds **1b**, **2b** and **3b**).

The introduction of the tyramine nucleus in place of one of the two naphthalenic moieties resulted in derivatives with activities comparable to those of their counterparts (cf. activities of **1a** and **4a**, or **1b** and **4b**). On the other hand, replacement with the isosteric indole-2-carboxylic moiety gave less homogeneous results. In fact, indolic derivatives **6a** and **6b** showed decreased RmtA inhibition (Table 1) in comparison with their naphthalenic counterparts **1a** and **1b**, respectively, but the activities against PRMT1 were similar (Table 1 and Table 2). Strangely, in this case, carboxylic acid **6b** was less active than the corresponding ester **6a**. This outcome could be justified by the formation of an intramolecular H bond between the indole NH and the COOH group, thus reducing the availability of both groups for interaction with the binding pocket of the enzyme.

Regarding compounds resulting from the formal shift of the ureidic function from the C-7 to the C-6 position of the naphthalene ring, it is noteworthy that their inhibitory activity was greatly enhanced. In fact, compounds **7**, **8**, and **9** were more potent than their positional isomers. Moreover, the biscarboxylic acid derivative **7b**, the isomer of **1b**, showed the highest inhibitory efficacy, comparable (Table 1) or even better (Table 2) than AMI-1.

Finally, the introduction of a tertiary amine, like the dimethylaminopropyl moiety in compound **5a**, led to a substantial decrease of the inhibitory potency against *h*PRMT1 (Table 2).

To determine whether the compounds that showed arginine methyltransferase inhibitory properties were able to inhibit PRMT activity within a cellular context, we used a fusion between green fluorescence protein (GFP) and the yeast protein Npl3. We previously established that mammalian PRMT1 can methylate Npl3 in vitro,[36] thus we reasoned that this reaction could also take place within a mammalian cell line. A destabilized GFP variant was used that displays rapid turnover rates. This shorter half-life makes destabilized variants suitable for use in quantitative reporter assays. The GFP–Npl3 was transiently transfected into HeLa cells; post-transfection the cells were treated for 24 h with derivatives **1b**, **7b**, **8b** and **9b** (10, 50, and 100 μM), using AMI-1 and 2′,3′-acycloadenosine-2′,3′-dialdehyde (adenosine dialdehyde, AdOx), an indirect methyltransferase inhibitor,[66,67] as reference compounds. Because GFP and Npl3 are fused, the αGFP antibody was used to establish equal loading and αNpl3 antibody (1E4)[68] acted as the methylation sensor (Figure 4A). Thus, the relative degree of arginine methylation in the presence of the different inhibitors can be established. Using this assay system we demonstrated that all tested derivatives were able to inhibit methylation of the GFP-Npl3 fusion, even if to varying extents (data not shown). We thus focused our attention on **7b**, the compound that showed the highest inhibitory efficacy in enzymatic assays. A concentration gradient of **7b** (10, 50, 100 μM) was used to treat GFP–Npl3 transiently transfected HeLa cells for 24 h, using AMI-1 (10 and 100 μM) and AdOx (10 and 20 μM) as reference compounds. Total cell extracts were then subjected to Western analysis with αGFP and 1E4 (methyl-sensitive αNpl3) antibodies. Derivative **7b** inhibited the methylation of Npl3 within the cell in a dose-dependent manner and more

Table 1. Inhibitory activities (IC_{50} values) of compounds **1**–**9** against *h*PRMT1 and RmtA using histone substrates.[a, b]

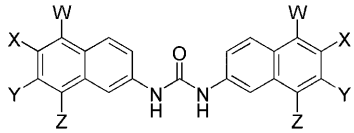

1a,**b**,**c** **7a**,**b**

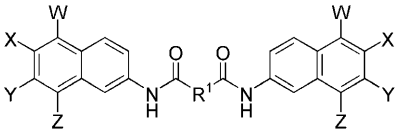

2a,**b** **3a**,**b** **8a**,**b**

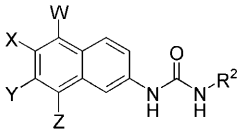

4a,**b** **5a**,**b** **6a**,**b** **9a**,**b**

Compd	W	X	Y	Z	R^1	R^2	$IC_{50} \pm SD$ [μM] RmtA	PRMT1
1a	OH	H	COOEt	H	–	–	190.8 ± 7.6	447.8 ± 19.9
1b	OH	H	COOH	H	–	–	137.7 ± 4.1	298.0 ± 8.9
1c	OH	H	$CONH_2$	H	–	–	445.1 ± 26.7	405.9 ± 20.3
2a	OH	H	COOEt	H	CH_2	–	121.0 ± 3.6	233.2 ± 9.3
2b	OH	H	COOH	H	CH_2	–	ND[c]	ND[c]
3a	OH	H	COOEt	H	CH_2CH_2	–	272.2 ± 10.9	676.1 ± 33.8
3b	OH	H	COOH	H	CH_2CH_2	–	122.8 ± 6.2	342.7 ± 17.2
4a	OH	H	COOEt	H	–	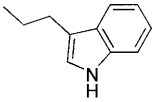	195.7 ± 7.8	345.6 ± 6.9
4b	OH	H	COOH	H	–	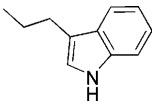	170.1 ± 8.5	262.3 ± 13.1
5a	OH	H	COOEt	H	–	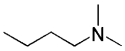	180.2 ± 3.6	875.0 ± 35.0
6a	OH	H	COOEt	H	–	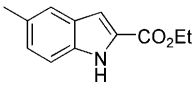	620.0 ± 24.8	510.0 ± 30.6
6b	OH	H	COOH	H	–	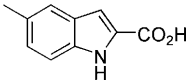	329.8 ± 16.5	0[d]
7a	H	COOMe	H	OH	–	–	204.3 ± 8.2	195.2 ± 7.8
7b	H	COOH	H	OH	–	–	94.7 ± 3.8	111.7 ± 3.4
8a	H	COOMe	H	OH	CH_2	–	204.9 ± 12.3	132.8 ± 5.3
8b	H	COOH	H	OH	CH_2	–	395.1 ± 15.8	271.6 ± 13.6
9a	H	COOMe	H	OH	–	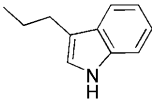	290.0 ± 14.5	320.2 ± 12.8
9b	H	COOH	H	OH	–	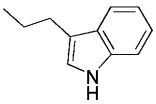	226.7 ± 9.1	205.4 ± 8.2
AMI-1	OH	H	SO_3H	H	–	–	88.2 ± 2.6[e]	92.1 ± 3.7[e]

[a] Chicken erythrocyte core histones and SAM were used as substrates at the concentration of 25 μM and 0.13 μM, respectively; [b] Values are means determined for at least two separate experiments; [c] Not determined; [d] No inhibition at 230 μM; [e] Literature value (Reference [41]): 33.2 ± 7.8 μM (RmtA) and 1.2 ± 0.5 μM (PRMT1), fluorescence assay.

effectively than the reference AMI-1 (Figure 4b). In addition, the inhibitor of global methylation, AdOx, also reduced the methylation status of this reporter.

Inhibition against a panel of arginine methyltransferases

The most active derivatives were selected and tested at 50 μM against a panel of arginine methyltransferases, as well as against a lysine methyltransferase, to assess their selectivity. Compounds **1b**, **1c**, **2b**, **4a**, **4b**, **7b**, **8b**, **9a**, and **9b** were tested against the human recombinant arginine methyltransferases PRMT1, PRMT3, CARM1 and PRMT6, using histone H4, GAR motifs and histone H3 (for both CARM1 and PRMT6) as substrates, respectively, and also against the lysine methyltransferase SET7/9, using histone H3 as a substrate. AMI-1 was used as reference compound in all assays.

As seen in Table 3, all of the derivatives tested are generally more selective for arginine methyltransferases than AMI-1. In fact, they are practically inactive against the lysine methyltransferase SET7/9, whereas AMI-1 shows a minor inhibition of this HKMT enzyme. This, together with its capability to inhibit all tested PRMTs, support the pleiotropic nature of the interactions established by the sulfonic groups.

In contrast, compound **1b**, the carboxylic analogue of AMI-1, is inactive against SET7/9 but its activity is fairly comparable to that of its sulfonic counterpart against PRMT3, and to a lesser

Table 2. Inhibitory activities of compounds **1**–**9** against *h*PRMT1 using nonhistone substrates.[a,b]

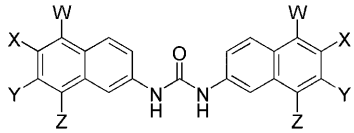

1a,**b**,**c** **7a**,**b**

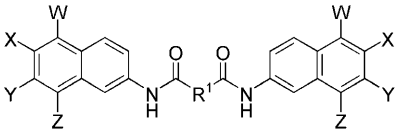

2a,**b** **3a**,**b** **8a**,**b**

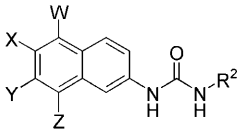

4a,**b** **5a**,**b** **6a**,**b** **9a**,**b**

Compd	W	X	Y	Z	R^1	R^2	inhibition [%] (hPRMT1/Npl3) 50 μM	10 μM
1a	OH	H	COOEt	H	–	–	40.81	4.91
1b	OH	H	COOH	H	–	–	75.16	41.73
1c	OH	H	$CONH_2$	H	–	–	63.47	0.13
2a	OH	H	COOEt	H	CH_2	–	34.65	10.77
2b	OH	H	COOH	H	CH_2	–	60.22	21.73
3a	OH	H	COOEt	H	CH_2CH_2	–	31.66	0.92
3b	OH	H	COOH	H	CH_2CH_2	–	30.85	-0.41
4a	OH	H	COOEt	H	–	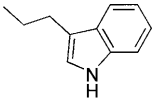	61.24	30.21
4b	OH	H	COOH	H	–	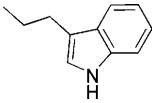	71.65	20.21
5a	OH	H	COOEt	H	–	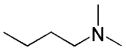	−7.20	−1.70
6a	OH	H	COOEt	H	–	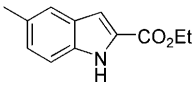	53.20	27.73
6b	OH	H	COOH	H	–	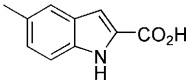	32.47	8.01
7a	H	COOMe	H	OH	–	–	59.07	19.62
7b	H	COOH	H	OH	–	–	100.00	75.29
8a	H	COOMe	H	OH	CH_2	–	52.07	25.13
8b	H	COOH	H	OH	CH_2	–	90.99	−8.59
9a	H	COOMe	H	OH	–	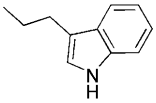	83.78	20.47
9b	H	COOH	H	OH	–	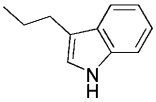	73.17	20.15
AMI-1	OH	H	SO_3H	H	–	–	100.00	66.89

[a] Npl3p was used as a nonhistone substrate, SAM as a cofactor (see Experimental Section); [b] Values given are means determined for at least two separate experiments.

degree against CARM1. Interestingly, the use of histone H4 instead of core histones or the nonhistone protein Npl3p as a substrate for the PRMT1 assay yielded an appreciably weaker inhibition of PRMT1. The malonic bisamidic derivative **2b** exhibited a similar activity profile against the enzyme panel (Table 3).

The bisamide **1c** was consistently less active than **1b** and **2b** against both PRMT3 and CARM1, but was the only compound among those tested that was able to inhibit PRMT6, with a potency comparable to that of AMI-1 or even higher. Regarding compound **7b**, the positional isomer of **1b**, this compound was confirmed as the most active in the series showing very good inhibitory activities against PRMT1, PRMT3, and CARM1, and was comparable or even better than that exhibited by AMI-1. However, it was practically inactive against both PRMT6 and SET7/9 (Table 3).

The bisamidic malonic analogue **8b** was consistently less active than **7b** against both PRMT1 and PRMT3, yet displayed a positive modulating effect on the enzymatic activity of CARM1 (Table 3). Similarly, the tryptamine derivatives **9a,b** showed little or no activity against PRMT1, PRMT3 and PRMT6, but strongly increased enzymatic activity of CARM1. In contrast, the isomeric derivatives **4a,b** showed only weak inhibition against all enzymes (see Supporting Information for fluorographs[69]).

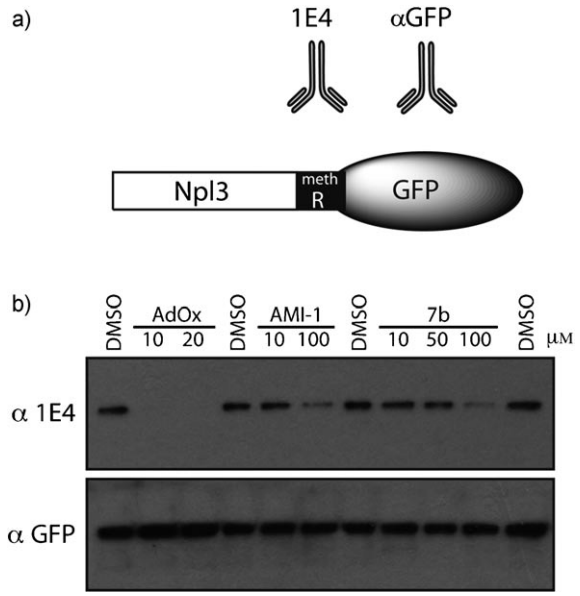

Figure 4. Effects of compounds on cellular arginine methyltransferase activity: a) a depiction of the GFP–Npl3 fusion protein with the position of methylated region and the antibodies that recognize it; b) HeLa cells were grown in 12-well plates and then transiently transfected with d2GFP–Npl3. Three hours post-transfection, the cells were incubated with the indicated compounds for 24 h. The cells were lysed in RIPA buffer, and Western analysis was performed with either the 1E4 antibody (top panel) or αGFP antibody (bottom panel). The effects of the compounds on GFP-Npl3 methylation status were established with the methyl-specific antibody, 1E4. The αGFP antibody showed the protein levels of GFP-Npl3. DMSO (0.25% *v/v*) was used as a vehicle (lanes 1, 4, 7, 11); compounds concentrations: AdOx (10 and 20 μM, lane 2,3), AMI-1 (10 and 100 μM, lanes 5,6), **7b** (10, 50, and 100 μM, lanes 8–10).

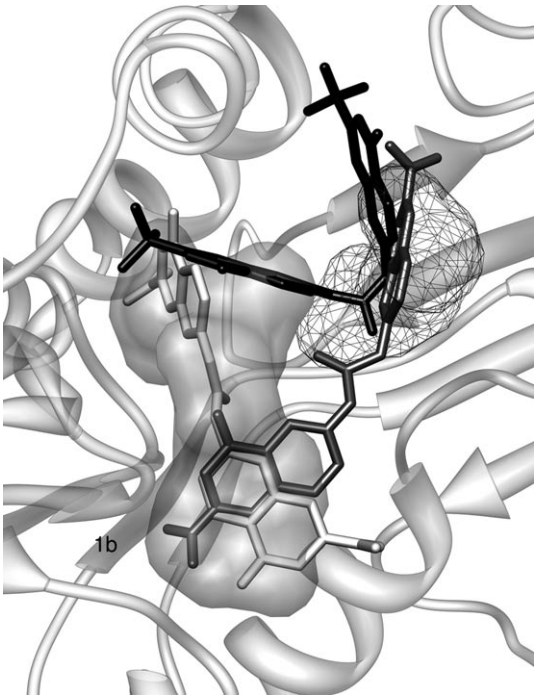

Figure 5. Autodock/X-Score selected binding conformations of compounds **1b** (light gray), **7b** (dark gray) and AMI-1 (black) docked into the RmtA catalytic site. The volumes occupied by Arg and SAM are represented in mesh and filled transparent gray, respectively.

Binding mode studies

The binding modes of selected PRMT inhibitors were studied in an attempt to rationalize the differences in activity. To this aim, compounds **1b**, **7b**, and AMI-1 were docked (Autodock 3)[70] into the homology model of the PRMT1 orthologue RmtA, previously reported by us[40] and used to describe three different binding modes of PRMT inhibitors: a) molecules docked in the arginine pocket (DAP); b) molecules docked in the SAM pocket (DSP); and c) molecules partially overlapping with both sites (docked in both pockets, DBP).[40] The analysis of the Autodock conformations selected by the X-Score[71] external scoring function showed that **1b** belongs to the DSP group, while **7b** seems to bind in both sites and so belongs to the DBP group (Figure 5).

In particular, the binding conformation selected for **1b** is similar to the one observed for the SAM co-factor (Figure 6). In fact, one naphthalenic group lays in a

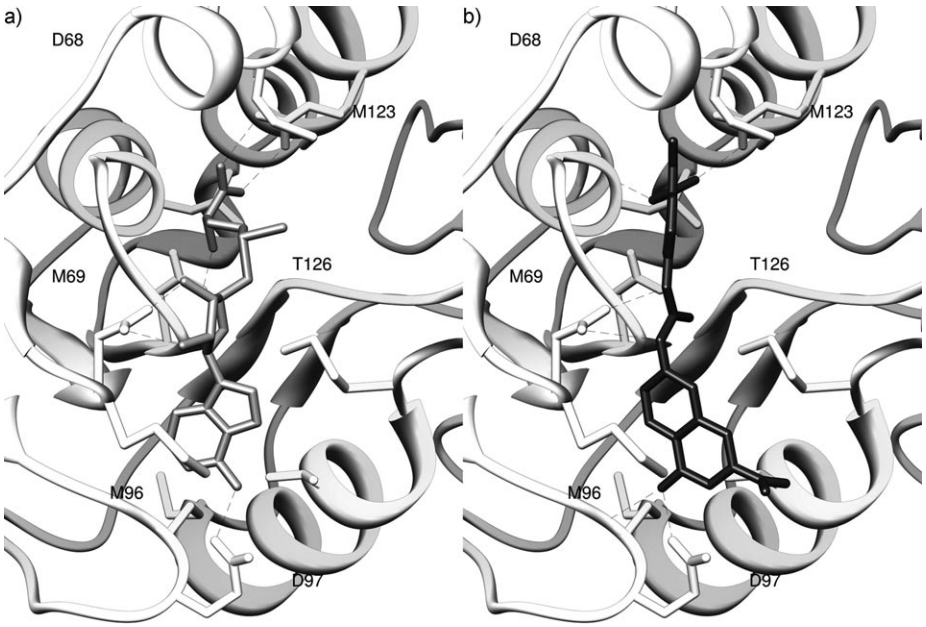

Figure 6. Comparison between binding conformations of SAM cofactor and compound **1b** in the RmtA catalytic site. a) SAM cofactor (light gray carbon atoms); b) **1b** (dark gray carbon atoms). The RmtA residues within 4.0 Å from the docked compounds are reported in white. For the sake of clarity, hydrogen atoms are not displayed.

Table 3. Inhibition activities of selected compounds against different methyltransferases.[a]

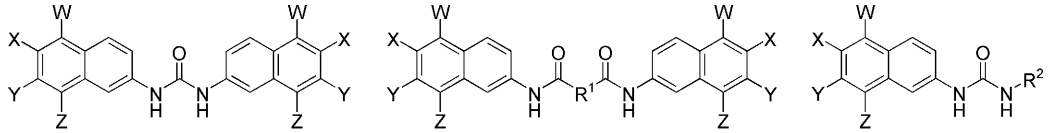

1b,**c** **7b** **2b** **8b** **4a**,**b** **9a**,**b**

Compd	W	X	Y	Z	R^1	R^2	Inhibition [%] at 50 μM				
							PRMT1/H4[b]	PRMT3/GAR[c]	CARM1/H3[d]	PRMT6/H3[d]	SET7/9/H3[d]
1b	OH	H	COOH	H	–	–	12.36	90.92	53.06	−7.23	−8.07
1c	OH	H	$CONH_2$	H	–	–	42.42	29.46	9.26	43.77	13.36
2b	OH	H	COOH	H	CH_2	–	48.44	91.94	54.96	6.40	−1.40
4a	OH	H	COOEt	H	–	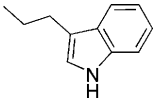	24.73	42.13	−46.56	−12.40	6.65
4b	OH	H	COOH	H	–	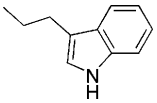	9.86	13.98	39.53	18.30	−5.13
7b	H	COOH	H	OH	–	–	61.65	72.81	83.07	−21.72	3.80
8b	H	COOH	H	OH	CH_2	–	16.76	32.56	−298.99	−2.09	14.44
9a	H	COOMe	H	OH	–	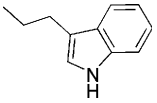	20.50	−5.03	−328.49	9.70	−8.46
9b	H	COOH	H	OH	–	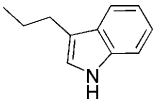	38.89	−8.17	−217.98	−11.13	−10.41
AMI-1	OH	H	SO_3H	H	–	–	87.67	101.33	74.76	40.69	34.34

[a] Values given are means determined for at least two separate experiments; [b] Histone H4 (1.5 μM) and SAM (0.42 μM) were used as substrates; [c] Glycine- and arginine-rich (GAR) motifs (0.41 μM) and SAM (0.42 μM) were used as substrates; [d] Histone H3 (1.1 μM) and SAM (0.42 μM) were used as substrates.

sandwich-like mode between the Met 69 and Met 123 side chains (SAM adenine binding site) making positive van der Waals interactions, while the corresponding carboxylate group makes a weak H bond with the hydroxy group of Thr 126. The other aromatic moiety binds in the SAM methionine pocket, delimited by Arg 22, Asp 44, Gly 46, Cys 47, Ile 51, Leu 52 and Glu 112, and the carboxylate function establishes either an electrostatic or a H-bond interaction with the Arg 22 side chain. Moreover, the two ureidic NH are within H bonding distance of the Asp 68 carboxylate group (Figure 6b), thus mimicking the two hydroxy groups of the SAM ribosyl moiety (cf. Figure 6a and 6b).

Notably, derivative **7b** displays a substantially different binding scenario from the one described above for its positional isomer **1b**, as the binding conformation selected by X-Score shows it belongs to the DBP group (Figure 7). Significant H bonds may be observed between **7b** and both arginine-anchoring residues Glu 112 and Glu 121 and Asp 68 (Figure 7b).

The differences in affinity values among derivatives that are highly structurally related (like **1b**, **7b** and AMI-1) could be better highlighted by direct comparison of their respective binding modes while maintaining the same protein orientation (Figure 8), and by comparison of the bonding interactions (Table 4) made by each inhibitor with the residues in the RmtA binding pockets.

Table 4. Summary report of the interactions between AMI-1, **7b**, **1b** and RmtA amino acid residues.

AMI-1		**7b**		**1b**	
d [Å]	residue•••••substituent	d [Å]	residue•••••substituent	d [Å]	residue•••••substituent
Electrostatic/H-bond interactions					
2.9	Glu 15•••••OH				
3.1	Arg 22•••••SO_3^{2-}			2.7	Arg 22•••••CO_2^-
2.9	His 261•••••SO_3^{2-}	3.2	His261•••••CO_2^-		
		3.2	Tyr116•••••CO_2^-		
3.3	Met 114•••••NH				
2.8	Glu 112•••••NH	3.6	Glu112•••••OH		
		2.8	Glu121 NH		
2.7	Thr 49 NH•••••SO_3^{2-}				
		2.9	Asp 68•••••OH	2.8	Asp68•••••NH
		2.7	Met 96-NH•••••CO_2^-	2.8	Met96-NH•••••OH
				2.3	Glu 97•••••OH
				3.3	Leu 52-NH•••••CO_2^-
				2.9	Tyr 126•••••CO_2^-
Hydrophobic interactions					
Met 16-Thr 49-Gly 46		–		Met16-Thr49-Gly46	
Trp262-His261-Tyr116		Trp 262-His 261-Tyr 116		–	
–		Met 123-Met 69		Met 123-Met 69	

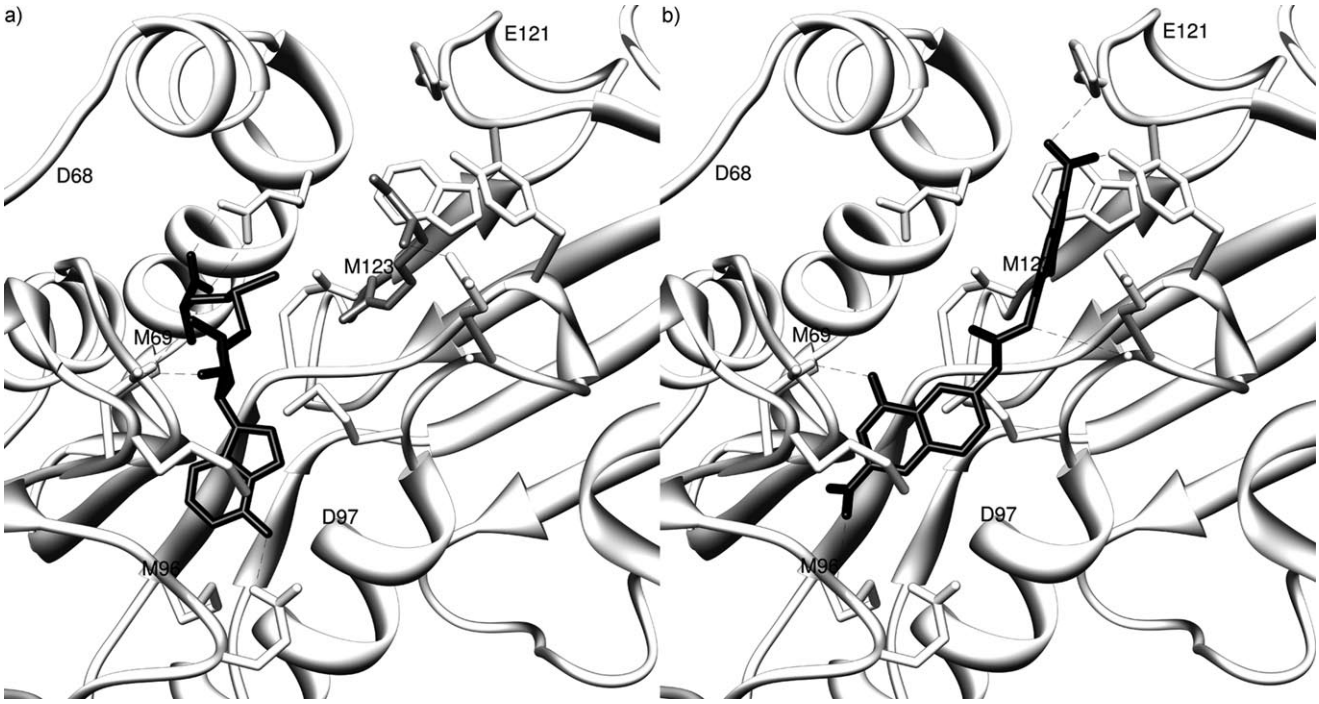

Figure 7. Binding conformations of compound **7b** in the RmtA catalytic site. a) SAM cofactor (dark gray carbon atoms) and arginine substrate (light gray carbon atoms); b) **7b** (dark gray carbon atoms). The RmtA residues within 4.0 Å from the docked compounds are reported in white. For the sake of clarity, hydrogen atoms are not displayed.

Like AMI-1, derivative **7b** can be classified as a DBP binding compound, even though it shows a stretched conformation, while AMI-1 was found to bind in a bent shape. In fact, similar to AMI-1, half of **7b** structure is buried in a hydrophobic pocket delimited by Trp 262, His 261, and Tyr 116 side chains. However, the second half of **7b** is located in the SAM adenine binding pocket, while the second half of AMI-1 is placed into the SAM methionine site.

On the other hand, **1b** is a DSP binding derivative and thus shares fewer interactions with AMI-1 than **7b** does. Interestingly, the binding profile of **1b** seems to be intermediate between those displayed by **7b** and AMI-1. In fact, half of its structure is docked in the SAM methionine site, similar to AMI-1, and the other half occupies the same SAM adenine binding region that is also filled by a **7b** naphthyl group (Figures 5 and 8).

In all three derivatives, either sulfonic or carboxylic acid groups act as anchoring points to the protein establishing relevant interactions. In particular, one AMI-1 sulfonic group interacts with Arg 22 (guanidinic side chain) and Thr 49 (amidic NH) (Table 4), and the second with main chain His 261 amidic NH. On the other hand, **1b** and **7b** carboxylic groups, while sharing some interactions with the AMI-1 sulfonic group (H bonds with Arg 22 and His 261 for **1b** and **7b**, respectively, Table 4), establish new interactions with either Tyr 116 and Met 96 (**7b**) or Leu 52 and Tyr 126 (**1b**).

A deeper analysis of the binding modes described above could help explain the observed activity trend. The lower activity of **1b** with respect to those observed for **7b** and AMI-1 could be due to its weaker interaction with the important Ile 12-His 13-His 16-Thr 49 pocket, as well as to the lack of any interaction with the arginine-anchoring residues Glu 112 and Glu 121, which seem to play an important role in the enzyme inhibition.

This scenario is also supported by the X-Score protein–ligand complex binding affinity estimations calculated by the HMScore (hydrophobic matching algorithm), which correlates with the IC_{50} values (Supporting Information, table B). Considering the HMScore, when a hydrophobic ligand atom is placed in a hydrophobic site of a protein, it is expected to contribute favorably to the binding process. As a matter of fact, AMI-1 and **7b** present higher hydrophobic matching values than **1b**, which contributes positively to the protein–ligand binding process and consequently to the activity (Supporting Information, table B).

Conclusions

We started by stating the rationale by which 7,7′-carbonylbis-(azanediyl)bis(4-hydroxynaphthalene-2-sulfonic acid) (AMI-1), a selective PRMT inhibitor[36] with a bisanionic structure that is related to compounds known to generate pleiotropic interactions with many proteins, should be further optimized before exploring additional binding pockets. On the basis of these observations, we have described the synthesis of compounds **1**–**9**, which are structurally related to AMI-1 and are characterized by the substitution of the sulfonic groups with the bioisosteric carboxylic groups, the replacement of the ureidic function with a bisamidic moiety, the introduction of a N-containing

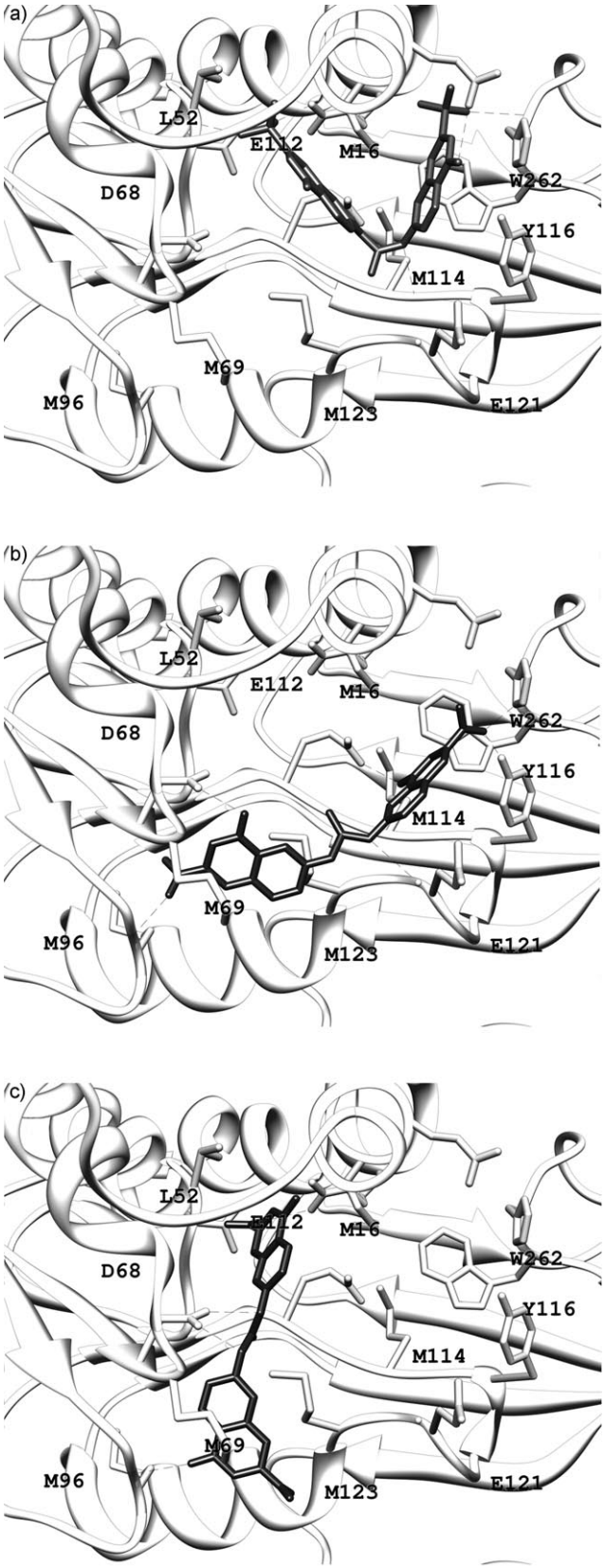

Figure 8. Comparison between binding conformations of a) AMI-1, b) **7b** and c) **1b** in the RmtA catalytic site. The RmtA residues within 4.0 Å from the docked compounds are reported in white. For the sake of clarity, hydrogen atoms are not displayed.

basic moiety or the positional isomerization of the aminohydroxynaphthoic moiety. We assessed their biological activity against a panel of arginine methyltransferases (fungal RmtA, *h*PRMT1, *h*CARM1, *h*PRMT3, *h*PRMT6), as well as against SET7/9 lysine methyltransferase, using histone and nonhistone proteins as substrates.

Preliminary structure–activity relationships were obtained from the biological data. Substitution of the AMI-1 sulfonic group with the carboxylic isoster gave compound **1b**, which maintained a fairly good activity. Moreover, derivatives resulting from the formal shift of the ureidic function from the C-7 to the C-6 position of the naphthalene ring (compounds **7**, **8**, and **9)** were more potent than their positional isomers. The biscarboxylic acid **7b**, an isomer of **1b**, showed the highest inhibitory efficacy in vitro and was able to prevent arginine methylation of cellular proteins in whole-cell assays, with activities comparable or even better than AMI-1.

All derivatives evaluated were found to be selective for arginine methyltransferases, and practically inactive against the lysine methyltransferase SET7/9, whereas AMI-1, due to the pleiotropic nature of the interactions established by the sulfonic groups, inhibits all the enzymes tested, albeit with different potencies, including a minor inhibition of the HKMT SET7/9.

To rationalize the observed differences in terms of activity, we also performed molecular modeling studies that yielded a deep binding mode analysis of tested molecules. In both derivatives **1b** and **7b** the carboxylic acid groups act as anchoring points to the protein by establishing relevant interactions. In particular, while sharing some common interactions with the AMI-1 sulfonic groups (H bonds with Arg 22 and His 261 for **1b** and **7b**, respectively), they establish new interactions with either Tyr 116 and Met 96 (**7b**), or Leu 52 and Tyr 126 (**1b**). Moreover, derivative **7b** presents higher hydrophobic matching values than **1b**, which contributes positively to the protein–ligand binding process and to activity. Consequently it emerged as a promising candidate for further derivatization, and represents a step towards potent and selective arginine methyltransferase inhibitors.

Experimental Section

Chemistry

All chemicals were purchased from Aldrich Chimica (Milan, Italy) or from Alfa Aesar GmbH (Karlsruhe, Germany) and were of the highest purity. All solvents were reagent grade and, when necessary, were purified and dried by standard methods. All reactions requiring anhydrous conditions were conducted under a positive atmosphere of nitrogen in oven-dried glassware. Standard syringe techniques were used for anhydrous addition of liquids. All microwave reactions were conducted using a CEM Corporation (Cologno al Serio, Italy) Discover LabMate system using the standard 10 mL reaction vessel. Reactions were routinely monitored by TLC performed on aluminum-backed silica gel plates (Merck DC, Alufolien Kieselgel 60 F_{254}) with spots visualized by UV light ($\lambda = 254$, 365 nm) or using a $KMnO_4$ alkaline solution. Solvents were removed using a rotary evaporator operating at a reduced pressure of ~10 Torr. Organic solutions were dried over anhydrous Na_2SO_4. Chromatographic separations were performed on silica gel (silica

gel 60, 0.063–0.200 mm; Merck DC) or on alumina (aluminum oxide 90, active, neutral, 0.063–0.200 mm; Merck DC) columns. Melting points were determined on a Gallenkamp melting point apparatus in open capillary tubes and are uncorrected. Infrared (IR) spectra (KBr) were recorded on a Shimadzu FTIR-8000 instrument. ^{1}H NMR spectra were recorded at 300 MHz on a Bruker Avance 300 spectrometer. Chemical shifts are reported in δ (ppm) relative to the internal reference tetramethylsilane (TMS). Mass spectra were recorded on a Finnigan LCQ DECA TermoQuest (San Jose, USA) mass spectrometer using an electrospray ion source (ESI-MS). Combustion analyses were performed by our Analytical Laboratory at the University of Salerno (Italy). All compounds showed $\geq$98% purity. When the elemental analysis is not included, crude compounds were used in the next step without further purification. As a rule, samples prepared for physical and biological studies were dried in high vacuum over P_2O_5 for 20 h at temperatures ranging from 25 to 110 °C, depending on the sample melting point.

Ethyl 7-amino-4-hydroxy-2-naphthoate (12a): A solution of **12a** and **12b** (3.00 g, 12.97 mmol), obtained as previously described,[60] in CH_3OH (150 mL) was treated dropwise with a solution of cobalt(II) acetate tetrahydrate (4.00 g, 16.06 mmol) in AcOH/AcONa pH 5 buffer (20 mL) over 30 min. The resulting slurry was heated at 50 °C for 3 h and then left at RT for an additional 3 h. The black solid was filtered off and the solution was concentrated in vacuo. Saturated aq $NaHCO_3$ (150 mL) was added to the resulting oil and the mixture was extracted with EtOAc (3×75 mL). The organic phase was dried, filtered and concentrated in vacuo to give **12a** as a white solid (0.96 g, 33%); mp: 245.5–246.5 °C (dec); ^{1}H NMR ($CDCl_3$): δ=10.57 (s, 1H), 8.03 (d, J=8.0 Hz, 1H), 7.92 (d, J=1.2 Hz, 1H), 7.18 (d, J=1.2 Hz, 1H), 7.02–6.96 (m, 2H), 5.50 (br s, 2H), 4.40 (q, J=7.3 Hz, 2H), 1.41 (t, J=7.3 Hz, 3H); MS (ESI): m/z: 232 $[M+H]^+$.

Diethyl 7,7′-carbonylbis(azanediyl)bis(4-hydroxy-2-naphthoate) (1a): Diphenylcarbonate (0.463 g, 2.16 mmol) and DMAP (0.053 g, 0.43 mmol) were added to a solution of **12a** (1.0 g, 4.32 mmol) in chlorobenzene (20 mL) and the mixture was refluxed for 72 h. The solvent was removed in vacuo, and the residue was washed with petroleum benzene (2×20 mL). The crude was dissolved in EtOAc (100 mL) and washed with 3 N aq HCl (3×70 mL). The organic phase was washed with brine, dried, filtered and concentrated in vacuo. Purification by column chromatography on silica gel (CH_2Cl_2/CH_3OH, 98:2→90:10) gave **1a** as a white solid (0.633 g, 60%); mp: 266.2–266.8 °C (dec); ^{1}H NMR ([D$_6$]DMSO): δ=10.43 (s, 2H), 9.11 (s, 2H), 8.16 (s, 2H), 8.10 (d, J=8 Hz, 2H), 7.94 (s, 2H), 8.33 (d, J=8 Hz, 2H), 7.25 (s, 2H), 6.45 (q, J=14 Hz, 4H), 1.36 (t, J=14 Hz, 6H); MS (ESI): m/z: 489 $[M+H]^+$; Anal. calcd for $C_{27}H_{24}N_2O_7$: C 66.39, H 4.95, N 5.73, found: C 66.52, H 4.94, N 5.72.

7,7′-Carbonylbis(azanediyl)bis(4-hydroxy-2-naphthoic acid) (1b): Pyridine (1.22 mmol, 98 μL) was added to a solution of ester **1a** (0.3 g, 0.61 mmol) in THF (4 mL). The reaction was treated dropwise with aq 1 N NaOH (12 mL) and the mixture was stirred at RT until starting material disappeared (silica TLC; AcOEt/AcOH, 99:1). THF was removed under a flow of N_2 and 2 N aq HCl (10 mL) was added. Filtration of the mixture gave **1b** as a white solid (0.260 g, 98%); mp: >290 °C; ^{1}H NMR ([D$_6$]DMSO): δ=10.37 (s, 2H), 9.09 (s, 2H), 8.13–8.10 (m, 4H), 7.93 (s, 2H), 7.67 (dd, J_1=9 Hz, J_2=1 Hz, 2H), 7.25 (d, J=1 Hz, 2H); MS (ESI): m/z: 433 $[M+H]^+$; Anal. calcd for $C_{23}H_{16}N_2O_7$: C 63.89, H 3.73, N 6.48, found: C 64.04, H 3.73, N 6.47. Acids **2b**, **3b**, **4b** and **6b** were obtained from the corresponding esters **2a**, **3a**, **4a**, and **6a**, respectively, following the same procedure.[62]

7-(3-(7-Carboxy-5-hydroxynaphthalen-2-ylamino)-3-oxopropanamido)-4-hydroxy-2-naphthoic (2b): White solid (96%); mp: >290 °C; ^{1}H NMR ([D$_6$]DMSO): δ=10.50 (s, 2H), 10.45 (s, 2H), 8.33 (s, 2H), 8.14 (d, J=9 Hz, 2H), 7.93 (s, 2H), 7.73 (d, J=9 Hz, 2H), 7.29 (s, 2H), 3.64 (s, 2H); MS (ESI): m/z: 475 $[M+H]^+$; Anal. calcd for $C_{25}H_{18}N_2O_8$: C 63.29, H 3.82, N 5.90, found: C 63.38, H 3.82, N 5.89.

7-(4-(7-Carboxy-5-hydroxynaphthalen-2-ylamino)-4-oxobutanamido)-4-hydroxy-2-naphthoic (3b): White solid (90%); mp: >290 °C; ^{1}H NMR (D_2O+NaOD): δ=7.92 (d, J=9 Hz, 2H), 7.55 (d, J=9 Hz, 2H), 7.27 (s, 2H), 7.12–7.07 (m, 4H), 2.55 (s, 4H); MS (ESI): m/z: 489 $[M+H]^+$; Anal. calcd for $C_{26}H_{20}N_2O_8$: C 63.93, H 4.13, N 5.74, found: C 64.03, H 3.75, N 5.73.

7-(3-(2-(1*H*-Indol-3-yl)ethyl)ureido)-4-hydroxy-2-naphthoic (4b): White solid (98%); mp: >290 °C; ^{1}H NMR ([D$_6$]DMSO): δ=11.77 (s, 1H), 10.83 (s, 1H), 10.25 (s, 1H), 8.75 (s, 1H), 8.00 (d, J=7 Hz,1H), 7.98 (s, 1H), 7.81 (s, 1H), 7.57 (d, J=8 Hz, 1H), 7.53 (dd, J_1=9 Hz, J_2=2 Hz, 1H), 7.33 (d, J=8 Hz, 1H), 7.17 (d, J=2 Hz, 1H), 7.15 (d, J=1 Hz, 1H), 7.08–7.03 (m, 1H), 6.99–6.94 (m, 1H), 6.24 (t, J=12 Hz, 1H), 3.45–3.49 (m, 2H), 2.87 (t, J=14 Hz, 2H); MS (ESI): m/z: 390 $[M+H]^+$; Anal. calcd for $C_{22}H_{19}N_3O_4$: C 67.86, H 4.92, N 10.79, found: C 67.98, H 4.92, N 10.78.

5-(3-(7-Carboxy-5-hydroxynaphthalen-2-yl)ureido)-1*H*-indole-2-carboxylic (6b): White solid (70%); mp: >290 °C; ^{1}H NMR ([D$_6$]DMSO): δ=11.62 (s, 1H), 10.31 (s, 1H), 8.91 (s, 1H), 8.67 (s, 1H), 8.08–8.03 (m, 2H), 7.88–7.85 (m, 2H), 7.63 (d, J=8 Hz, 1H), 7.37 (d, J=8 Hz, 1H), 7.26 (s, 1H), 7.21 (s, 1H), 7.02 (s, 1H); MS (ESI): m/z: 406 $[M+H]^+$; Anal. calcd for $C_{25}H_{23}N_3O_6$: C 65.07, H 5.02, N 9.11, found: C 65.19, H 5.01, N 9.10.

7,7′-Carbonylbis(azanediyl)bis(4-hydroxy-2-naphthamide) (1c): A mixture of compound **1a** (0.3 g, 0.61 mmol) and NH_4OH (30% *w*/*w*, 20 mL) was stirred at RT for 12 h. The solution was then acidified to pH 5 with 3 N aq HCl and isolation of the light brown solid by filtration gave **1c** (0.157 g, 60%); mp: >290 °C; ^{1}H NMR ([D$_6$]DMSO): δ=10.23 (s, 2H), 9.13 (s, 2H), 8.15 (s, 2H), 8.07 (d, J=9 Hz, 2H), 7.98 (s, 2H), 7.81 (s, 2H), 7.54 (d, J=9 Hz, 2H), 7.31 (s, 2H), 7.18 (s, 2H); MS (ESI): m/z: 431 $[M+H]^+$; Anal. calcd for $C_{23}H_{18}N_4O_5$: C 64.18, H 4.22, N 13.02, found: C 64.29, H 4.21, N 13.00.

Ethyl 7-(3-ethoxy-3-oxopropanamido)-4-hydroxy-2-naphthoate (13): A suspension of **12a** (1.0 g, 4.32 mmol) in diethyl malonate (6.5 mL) was irradiated for 30 min at 300 W keeping the temperature below 100 °C (air flow cooling). EtOAc (100 mL) was added to the crude and the solution was washed with 6 N aq HCl (3×70 mL). The organic phase was dried, filtered and concentrated in vacuo. Purification by column chromatography on silica gel (CH_2Cl_2/CH_3OH, 99:1→95:5) gave **13** as a light yellow solid (1.34 g, 90%); mp: 201–202 °C; ^{1}H NMR ([D$_6$]DMSO): δ=10.47 (s, 1H), 10.44 (s, 1H), 8.29 (s, 1H), 8.10 (d, J=9 Hz, 1H), 7.92 (s, 1H), 7.64 (d, J=9 Hz, 1H), 7.27 (s, 1H), 4.32 (q, J=14 Hz, 2H), 4.12 (q, J=14 Hz, 2H), 3.51 (s, 2H), 1.34 (t, J=14 Hz, 3H), 1.20 (t, J=14 Hz, 3H); MS (ESI): m/z: 346 $[M+H]^+$.

Ethyl 7-(3-(7-(ethoxycarbonyl)-5-hydroxynaphthalen-2-ylamino)-3-oxopropanamido)-4-hydroxy-2-naphthoate (2a): Compound **12a** (0.740 g, 3.19 mmol) was added to a solution of **13** (1.00 g, 2.90 mmol) in toluene (10 mL) and 1-methyl-2-pyrrolidinone (1 mL). The mixture was irradiated (3×30 min) at 300 W keeping the temperature below 120 °C (air flow cooling). The reaction was concentrated in vacuo and redissolved in EtOAc (150 mL). The solution was washed with 1 N aq HCl (3×60 mL), dried, filtered and concen-

trated in vacuo. Purification by column chromatography on silica gel (CH_2Cl_2/CH_3OH, 99:1→90:10) gave **2a** as a white solid (0.770 g, 50%); mp: 282.2–282.7 °C; ^{1}H NMR ([D$_6$]DMSO): δ = 10.50 (s, 2H), 10.47 (s, 2H), 8.34 (s, 2H), 8.11 (d, J = 9 Hz, 2H), 7.92 (s, 2H), 7.70 (dd, J_1 = 9 Hz, J_2 = 1 Hz, 2H), 7.27 (s, 2H), 4.32 (q, J = 14 Hz, 4H), 3.61 (s, 2H), 1.33 (t, J = 14 Hz, 6H); MS (ESI): m/z: 531 $[M+H]^+$; Anal. calcd for $C_{29}H_{26}N_2O_8$: C 65.65, H 4.94, N 5.28, found: C 65.76, H 4.93, N 5.27.

Ethyl 7-(4-(7-(ethoxycarbonyl)-5-hydroxynaphthalen-2-ylamino)-4-oxobutanamido)-4-hydroxy-2-naphthoate (3a): A solution of **12a** (1.0 g, 4.32 mmol) in acetone (6 mL) was cooled to −15 °C and treated dropwise with a solution of succinyl dichloride (0.401 g, 2.59 mmol) in acetone (12 mL) over 30 min. The resulting solution was stirred for 12 h at RT, then aq $NaHCO_3$ (6 mL) was added and the mixture concentrated in vacuo. The crude oil was redissolved in aq $NaHCO_3$ (100 mL) and extracted with EtOAc (3×60 mL). The combined organic phases were washed with 2N aq HCl (3× 60 mL), dried, filtered and concentrated in vacuo to give a crude solid. Purification by flash chromatography on silica gel (CH_2Cl_2/ CH_3OH, 99:1→90:10) gave **3a** as a white solid (0.470 g, 40%); mp: >290 °C; ^{1}H NMR ([D$_6$]DMSO): δ = 10.50 (s, 2H), 10.37 (s, 2H), 8.33 (s, 2H), 8.07 (d, J = 9 Hz, 2H), 7.87 (s, 2H), 7.68 (d, J = 9 Hz, 2H), 7.31 (s, 2H), 4.31 (q, J = 21 Hz, 4H), 2.83 (s, 2H), 1.33 (t, J = 21 Hz, 6H); MS (ESI): m/z: 545 $[M+H]^+$; Anal. calcd for $C_{25}H_{23}N_3O_6$: C 65.07, H 5.02, N 9.11, found: C 65.15, H 5.01, N 9.10.

Ethyl 4-hydroxy-7-(2,2,2-trichloroacetamido)-2-naphthoate (14): Et_3N (0.674 g, 6.67 mmol) was added to a solution of **12a** (1.0 g, 4.32 mmol) in dry CH_2Cl_2 (100 mL) under a flow of N_2. After 30 min, trichloroacetylchloride (1.212 g, 6.67 mmol) was added dropwise over 10 min under a flow of N_2 and the reaction was stirred at RT for 4 h. The solution was then washed with saturated aq $NaHCO_3$ (3×40 mL) and 3N aq HCl (3×40 mL), then dried, filtered and concentrated in vacuo. Purification by column chromatography on silica gel (CH_2Cl_2/CH_3OH, 99:1→90:10) gave **14** as a light yellow solid (1.34 g, 83%); mp: 232.0–232.7 °C; ^{1}H NMR ([D$_6$]DMSO): δ = 11.06 (s, 1H), 10.56 (s, 1H), 8.29 (s, 1H), 8.16 (d, J = 9 Hz, 1H), 7.99 (s, 1H), 7.80 (d, J = 9 Hz, 1H), 7.33 (s, 1H), 4.34 (q, J = 14 Hz, 2H), 1.34 (t, J = 14 Hz, 3H); MS (ESI+): m/z (%): 376 (100) $[M+H]^+$, 378 (96) $[M+H+2]^+$, 380 (36) $[M+H+4]^+$, 382 (4) $[M+H+6]^+$.

Ethyl 7-(3-(2-(1*H*-indol-3-yl)ethyl)ureido)-4-hydroxy-2-naphthoate (4a): Na_2CO_3 (1.40 g, 13.25 mmol) and tryptamine (0.467 g, 2.91 mmol) were added to a solution of **14** (1.0 g, 2.65 mmol) in dry DMF (10 mL) and the resulting mixture was heated at 150 °C for 1 h in a sealed tube. The reaction was concentrated in vacuo and then redissolved in EtOAc (150 mL). The solution was then washed with 2N aq HCl (3×50 mL) and saturated aq $NaHCO_3$ (3× 50 mL), dried, filtered and concentrated in vacuo. Purification by column chromatography on silica gel (CH_2Cl_2/CH_3OH, 99:1→90:10) gave **4a** as a white solid (0.696 g, 63%); mp: 214.7–215.5 °C; ^{1}H NMR ([D$_6$]DMSO): δ = 10.82 (s, 1H), 10.39 (br s, 1H), 8.79 (d, J = 4 Hz, 1H), 8.03–7.99 (m, 2H), 7.84 (s, 1H), 7.59–7.51 (m, 2H), 7.34 (d, J = 9 Hz, 1H), 7.19–7.18, (m, 2H), 7.06–7.03 (m, 1H), 6.97–6.95 (m, 1H), 6.29 (t, J = 12 Hz, 1H), 4.31 (q, J = 14 Hz, 2H), 4.43–4.41 (m, 2H), 2.91 (t, J = 25 Hz, 2H), 1.33 (t, J = 14 Hz, 3H); MS (ESI): m/z: 418 $[M+H]^+$; Anal. calcd for $C_{24}H_{23}N_3O_4$: C 69.05, H 5.55, N 10.07, found C 69.14, H 5.54, N 10.06. Derivatives **5a** and **6a** were obtained following the same procedure starting from **14** and N^1,N^1-dimethylpropane-1,3-diamine or ethyl 5-amino-1*H*-indole-2-carboxylate, respectively, as the nucleophile.

Ethyl 7-(3-(2-(dimethylamino)propyl)ureido)-4-hydroxy-2-naphthoate (5a): White solid (63%); mp: 161–163 °C; ^{1}H NMR ([D$_6$]DMSO): δ = 10.36 (s, 1H), 8.76 (s, 1H), 8.03–8.00 (m, 2H), 7.85 (s, 1H), 7.55 (dd, J_1 = 9 Hz, J_2 = 1 Hz, 1H), 7.19 (s, 1H), 6.34 (t, J = 9 Hz, 1H), 4.33 (q, J = 14 Hz, 2H), 3.17–3.11 (m, 2H), 2.36–2.31 (m, 2H), 2.20 (s, 6H), 1.63–1.58 (m, 2H), 1.34 (t, J = 14 Hz, 3H); MS (ESI): m/z: 360 $[M+H]^+$; Anal. calcd for $C_{19}H_{25}N_3O_4$: C 63.49, H 7.01, N 11.69, found: C 63.57, H 7.00, N 11.67.

Ethyl 5-(3-(7-(ethoxycarbonyl)-5-hydroxynaphthalen-2-yl)ureido)-1*H*-indole-2-carboxylate (6a): White solid (50%); mp: 210.8–211.7 °C; ^{1}H NMR ([D$_6$]DMSO): δ = 11.74 (s, 1H), 10.39 (s, 1H), 8.98 (s, 1H), 8.75 (s, 1H), 8.17 (s, 1H), 8.08 (d, J = 9 Hz, 1H), 7.94–7.88 (m, 2H), 7.64 (d, J = 8 Hz, 1H), 7.39 (d, J = 8 Hz, 1H), 7.27 (d, J = 9 Hz, 1H), 7.23 (s, 1H), 7.07 (s, 1H), 4.35 (q, J = 13 Hz, 4H), 1.38–1.32 (m, 6H); MS (ESI): m/z: 462 $[M+H]^+$; Anal. calcd for $C_{25}H_{23}N_3O_6$: C 65.07, H 5.02, N 9.11, found: C 65.17, H 5.01, N 9.10.

(*E*)-3-(Methoxycarbonyl)-4-(4-nitrophenyl)but-3-enoic acid: Carboxyphosphorane **10**[61] (13.0 g, 35.2 mmol) was suspended in dry benzene (150 mL) and 4-nitrobenzaldehyde (5.74 g, 38.0 mmol) was then added. The resulting mixture was stirred at RT for 48 h and then extracted with saturated aq $NaHCO_3$ (3×70 mL). The aqueous phase was washed with Et_2O, acidified with concd HCl and the white solid formed was collected by filtration (8.60 g, 92%) and directly used in the following step without further purification; mp: 158–160 °C; ^{1}H NMR ([D$_6$]DMSO): δ = 8.30 (d, J = 9 Hz, 2H), 7.86 (s, 1H), 7.69 (d, J = 9 Hz, 2H), 3.78 (s, 3H), 3.43 (s, 2H); MS (ESI): m/z: 266 $[M+H]^+$.

Methyl 4-acetoxy-6-nitro-2-naphthoate (15): A round-bottomed flask containing a magnetic stirring bar and fitted with a reflux condenser was charged with a mixture of (*E*)-3-(methoxycarbonyl)-4-(4-nitrophenyl)but-3-enoic acid (5.0 g, 18.85 mmol), Ac_2O (35 mL) and NaOAc (2.30 g, 28.27 mmol). The flask was subjected to MW irradiation (power 300 W) for 5 min keeping temperature below 120 °C (air flow cooling). The reaction mixture was filtered and the filtrate was concentrated to give **15** as a yellow solid (5.17 g, 95%); mp: 167–168 °C; ^{1}H NMR ($CDCl_3$): δ = 8.89 (d, J = 2 Hz, 1H), 8.62 (s, 1H), 8.38 (dd, J_1 = 9 Hz, J_2 = 2 Hz, 1H), 8.17 (d, J = 9 Hz, 1H), 8.05 (s, 1H), 4.05 (s, 3H), 2.59 (s, 3H); MS (ESI): m/z: 290 $[M+H]^+$.

Methyl 4-acetoxy-6-amino-2-naphthoate (16): Pd/C (5 wt% on activated carbon, 0.1 equiv) was added to a solution of **15** (3.0 g, 10.37 mmol) in EtOH (100 mL) and the reaction was stirred under H_2 (1 atm, balloon) for 2 h. The reaction mixture was filtered and concentrated to give **16** as a light yellow solid (2.66 g, 99%); mp: 195–196 °C; ^{1}H NMR ([D$_6$]DMSO): δ = 8.28 (s, 1H), 7.86 (d, J = 9 Hz, 1H), 7.54 (s, 1H), 7.06 (d, J = 9 Hz, 1H), 6.79 (s, 1H), 6.04 (s, 2H), 3.87 (s, 3H), 2.42 (s, 3H); MS (ESI): m/z: 260 $[M+H]^+$.

Dimethyl 6,6′-carbonylbis(azanediyl)bis(4-hydroxy-2-naphthoate) (7a): Diphenylcarbonate (0.411 g, 1.92 mmol) and DMAP (0.046 g, 0.38 mmol) were added to a solution of **16** (1.0 g, 3.85 mmol) in chlorobenzene (20 mL) and the mixture was refluxed for 72 h. The solvent was removed in vacuo and the resultant dark brown solid was washed with petroleum benzene (2×20 mL). The crude was redissolved in EtOH (50 mL) and K_2CO_3 (0.585 g, 4.23 mmol) was added. The mixture was heated at 70 °C for 2 h, then concentrated and redissolved in EtOAc (100 mL). The organic phase was washed with 3N aq HCl (3×70 mL) and brine, dried, filtered and concentrated. Purification of the crude by column chromatography on silica gel (CH_2Cl_2/CH_3OH, 98:2→90:10) gave **7a** as a white solid (0.443 g, 50%); mp: 276.6–277.6 °C; ^{1}H NMR ([D$_6$]DMSO): δ = 10.39 (s, 2H), 9.13 (s, 2H), 8.42 (d, J = 2 Hz, 2H), 8.00 (s, 2H), 7.95 (d, J = 9 Hz, 2H), 7.56 (dd, J_1 = 9 Hz, J_2 = 2 Hz, 2H), 7.33 (s, 2H), 3.85 (s, 6H); MS (ESI): m/z: 461 $[M+H]^+$; Anal. calcd

for $C_{25}H_{20}N_2O_7$: C 65.21, H 4.38, N 6.08, found: C 65.29, H 4.37, N 6.07.

Acids **7b**, **8b** and **9b** were obtained from the corresponding esters **7a**, **8a**, and **9a**, respectively, following the same general procedure described above for compounds **1b**, **2b**, **3b**, **4b** and **6b**.

6,6′-Carbonylbis(azanediyl)bis(4-hydroxy-2-naphthoic acid) (7b): White solid (90%); mp: >290 °C; ^{1}H NMR ([D$_6$]DMSO): δ = 10.33 (s, 2H), 9.13 (s, 2H), 8.44 (d, J = 2 Hz, 2H), 8.00 (s, 2H), 7.96 (d, J = 9 Hz, 2H), 7.59 (dd, J_1 = 9 Hz, J_2 = 2 Hz, 2H), 7.35 (s, 2H); MS (ESI): m/z: 433 $[M+H]^+$; Anal. calcd for $C_{23}H_{16}N_2O_7$: C 63.89, H 3.73, N 6.48, found: C 63.95, H 3.73, N 6.47.

6-(3-(6-Carboxy-8-hydroxynaphthalen-2-ylamino)-3-oxopropanamido)-4-hydroxy-2-naphthoic acid (8b): White solid (85%); mp: >290 °C; ^{1}H NMR (CD$_3$OD): δ = 8.54 (d, J = 2 Hz, 2H), 8.09 (s, 2H), 7.91 (d, J = 9 Hz, 2H), 7.76 (dd, J_1 = 9 Hz, J_2 = 2 Hz, 2H), 7.39 (s, 2H), 3.51 (s, 2H); MS (ESI): m/z: 475 $[M+H]^+$; Anal. calcd for $C_{25}H_{18}N_2O_8$: C 63.29, H 3.82, N 5.90, found: C 63.38, H 3.81, N 5.89.

6-(3-(2-(1*H*-Indol-3-yl)ethyl)ureido)-4-hydroxy-2-naphthoic acid (9b): White solid (98%); mp: >290 °C; ^{1}H NMR ([D$_6$]DMSO): δ = 10.86 (s, 1H), 10.21 (s, 1H) 8.87 (s, 1H), 8.29 (d, J = 2 Hz, 1H), 7.94 (s, 1H), 7.86 (d, J = 9 Hz, 1H), 7.61 (d, J = 8 Hz, 1H), 7.53 (dd, J_1 = 9 Hz, J_2 = 2 Hz, 1H), 7.37 (d, J = 8 Hz, 1H), 7.30 (d, J = 1 Hz, 1H), 7.21 (d, J = 1 Hz, 1H), 7.09–7.05 (m, 1H), 7.00–6.95 (m, 1H), 6.24 (t, J = 12 Hz, 1H), 3.47–3.43 (m, 2H), 2.91 (t, J = 14 Hz, 2H); MS (ESI): m/z: 390 $[M+H]^+$; Anal. calcd for $C_{22}H_{19}N_3O_4$: C 67.86, H 4.92, N 10.79, found: C 67.96, H 4.91, N 10.78.

Methyl 4-acetoxy-6-(3-ethoxy-3-oxopropanamido)-2-naphthoate (17): Obtained from **16** (1.0 g, 3.85 mmol) following the same procedure described above for the preparation of **13**, to yield a white solid (1.30 g, 90%); mp: 170.5–171.9 °C; ^{1}H NMR ([D$_6$]DMSO): δ = 10.66 (s, 1H), 8.52 (s, 1H), 8.32 (s, 1H), 8.20 (d, J = 9 Hz, 1H), 7.80–7.76 (m, 2H), 4.16 (q, J = 14 Hz, 2H), 3.93 (s, 3H), 3.56 (s, 2H), 2.47 (s, 3H), 1.22 (t, J = 14 Hz, 3H); MS (ESI): m/z: 374 $[M+H]^+$.

Methyl 4-hydroxy-6-(3-(6-(methoxycarbonyl)-8-hydroxynaphthalen-2-ylamino)-3-oxopropanamido)-2-naphthoate (8a): Compound **16** (0.762 g, 2.94 mmol) was added to a solution of **17** (1,00 g, 2.68 mmol) in toluene (10 mL) and 1-methyl-2-pyrrolidinone (1 mL) and the mixture was irradiated (3×30 min) at 300 W, keeping temperature below 120 °C (air flow cooling). The reaction was concentrated in vacuo and redissolved in EtOAc (150 mL). The organic phase was washed with 1 N aq HCl (3×60 mL), dried, filtered and concentrated in vacuo. The crude residue was dissolved in EtOH (50 mL) and K_2CO_3 (0.407 g, 2.94 mmol) was added. The mixture was heated at 70 °C for 2 h, then concentrated and redissolved in EtOAc (100 mL). The organic phase was washed with 3 N aq HCl (3×70 mL) and brine, then dried, filtered and concentrated. Purification by column chromatography on silica gel (CH_2Cl_2/CH_3OH, 99:1→90:10) gave **8a** as a white solid (0.673 g, 50%); mp: 287.8–288.8 °C; ^{1}H NMR ([D$_6$]DMSO): δ = 10.51 (s, 2H), 10.44 (s, 2H), 8.55 (d, J = 2 Hz, 2H), 8.01 (s, 2H), 7.98 (d, J = 9 Hz, 2H), 7.73 (dd, J_1 = 9 Hz, J_2 = 2 Hz, 2H), 7.32 (s, 2H), 3.86 (s, 6H), 3.60 (s, 2H); MS (ESI): m/z: 503 $[M+H]^+$; Anal. calcd for $C_{27}H_{22}N_2O_8$: C 64.54, H 4.41, N 5.58, found: C 64.61, H 4.40, N 5.57.

Methyl 4-acetoxy-6-(2,2,2-trichloroacetamido)-2-naphthoate (18a) and methyl 4-hydroxy-6-(2,2,2-trichloroacetamido)-2-naphthoate (18b): Title compounds were obtained as a mixture starting from **16** (1.0 g, 3.85 mmol) following the same procedure described above for the preparation of **14**, to yield a crude white solid (1.14 g, 82%) that was directly used in the following step. For characterization purposes, analytical samples of **18a** and **18b** were obtained by column chromatography on silica gel (CH_2Cl_2/CH_3OH, 99:1→95:5); **18a**: mp: 162–163 °C; ^{1}H NMR ([D$_6$]DMSO): δ = 11.25 (s, 1H), 8.56 (s, 1H), 8.32 (s, 1H), 8.27 (d, J = 9 Hz, 1H), 8.03 (d, J = 9 Hz, 1H), 7.80 (s, 1H), 3.93 (s, 3H), 2.51 (s, 3H); MS (ESI): m/z: 404 $[M+H]^+$; **18b**: mp: 225–226 °C; ^{1}H NMR ([D$_6$]DMSO): δ = 11.13 (s, 1H), 10.63 (s, 1H), 8.55 (s, 1H), 8.07–8.05 (m, 2H), 7.85 (dd, J_1 = 9 Hz, J_2 = 2 Hz, 1H), 7.39 (s, 1H), 3.89 (s, 3H); MS (ESI): m/z: 362 $[M+H]^+$.

Methyl 6-(3-(2-(1*H*-indol-3-yl)ethyl)ureido)-4-hydroxy-2-naphthoate (9a): Prepared from a crude mixture of **18a** and **18b** (1.0 g, 2.77 mmol) following the same procedure described above for the preparation of **4a**, to yield a white solid (0.704 g, 63%); mp: 218.8–219.8 °C; ^{1}H NMR ([D$_6$]DMSO): δ = 10.83 (s, 1H), 10.26 (s, 1H), 8.87 (s, 1H), 8.26 (d, J = 2 Hz, 1H), 7.95 (s, 1H), 7.86 (d, J = 9 Hz, 1H), 7.57 (d, J = 8 Hz, 1H), 7.51 (dd, J_1 = 9 Hz, J_2 = 2 Hz, 1H), 7.33 (d, J = 8 Hz, 1H), 7.27 (s, 1H), 7.17 (d, J = 2 Hz, 1H), 7.06–7.03 (m, 1H), 6.97–6.93 (m, 1H), 6.22 (t, J = 12 Hz, 1H), 3.84 (s, 3H), 3.44–3.40 (m, 2H), 2.87 (t, J = 14 Hz, 2H); MS (ESI): m/z: 404 $[M+H]^+$; Anal. calcd for $C_{23}H_{21}N_3O_4$: C 68.47, H 5.25, N 10.42, found: C 68.58, H 5.24, N 10.41.

Biochemistry

Preparation of GST-RmtA and GST-PRMT1 fusion proteins

GST-PRMT1 fusion protein was expressed in *E. coli* BL21 cells. A culture of transformed *E. coli* BL21 cells was grown overnight in 10 mL of lysogeny broth (LB)[72] with ampicillin (100 μg mL^{-1}). Fresh LB (100 mL) with antibiotic was added and the culture was agitated for 1 h at 37 °C. Then *iso*-propyl-β-D-1-thiogalactopyranoside (IPTG) was added to give a final concentration of 0.1 mM, followed by additional shaking at 30 °C for 4 h. The bacterial culture was then centrifuged at 5000 rpm for 5 min at 4 °C, and the supernatant was discarded. The pellet was resuspended in 500 μL of cold PBS (137 mM NaCl, 2.7 mM KCl, 4.3 mM Na_2HPO_4, 1.4 mM KH_2PO_4, pH 7.4) and sonicated for 30 s. The suspension was spun down at 5000 rpm for 10 min at 4 °C. During that time, glutathione sepharose beads (GE Healthcare) were washed once with ice-cold PBS, then 100 μL of clean beads were placed into a 1.5 mL microcentrifuge tube and the supernatant added; the beads are rocked for 3–5 h at 4 °C. The beads were washed three times with ice-cold PBS. Fresh glutathione-reduced buffer was prepared by mixing elution buffer (100 mM Tris-HCl, pH 8.0; 120 mM NaCl) with glutathione reduced (0.01 g mL^{-1}). Glutathione-reduced buffer (100 μL) was added to the beads and rocked for 2 h at 4 °C. Finally, the beads were spun down and the supernatant collected.

The RmtA coding sequence[64] was cloned into a pGEX-5X-1 expression vector (GE Healthcare). RmtA protein was expressed in BL21 cells in LB medium. 250 mL cultures (A_{600} = 0.4) were induced with a final concentration of 1 mM IPTG and grown for 4 h at 37 °C. After centrifugation of cells at 4000 *g*, the pellet was resuspended in 6 mL of GST-binding buffer (140 mM NaCl, 2.7 mM KCl, 10 mM Na_2HPO_4, 1.8 mM KH_2PO_4, pH 7.3) containing one protease inhibitor tablet (Complete, Roche, Mannheim, Germany) per 50 mL of buffer. For cell lysis, lysozyme was added at a final concentration of 5 mg mL^{-1} binding buffer and cells were passed through a French press with pressure setting of 1000 psi. The resulting lysate was centrifuged at 20000 *g* for 10 min at 4 °C. GST fusion protein was purified from soluble extracts by binding to a GST-HiTrap column (GE Healthcare). Proteins were eluted with 50 mM Tris-HCl, 10 mM

reduced glutathione, pH 8.0 and assayed for histone methyltransferase activity.

GST-PRMT3, GST-PRMT4, and GST-PRMT6 have been described previously.[73] Unless stated otherwise, all chemicals/reagents were purchased from Sigma–Aldrich.

Protein methyltransferase assays

RmtA and PRMT1 (histone substrate) inhibitory assays and determination of IC_{50} values: For inhibition assays and determination of IC_{50} values, affinity-purified GST-RmtA and GST-PRMT1 fusion proteins were used as the enzyme source. HMT activities were assayed as described previously[64] using chicken erythrocyte core histones as substrate. GST-RmtA and GST-PRMT1 fusion proteins (500 ng) were incubated with five different concentrations of each compound for 15 min at RT and 2.5 μL of chicken core histones (8 mg mL^{-1}) and 1 μL of [^{3}H]-S-adenosyl-L-methionine ([^{3}H]SAM, 0.55 μCi) were added, resulting in concentrations of 25 and 0.13 μM, respectively. This mixture was incubated for 30 min at 30 °C. The reaction was stopped by TCA precipitation (25% final concentration) and samples were kept on ice for 20 min. Whole sample volumes were collected onto a glass fiber filter (Whatman GF/F) preincubated with 25% TCA. Filters were washed three times with 3 mL of 25% TCA and then three times with 1 mL of EtOH. After drying the filters for 10 min at 70 °C, radioactivity was measured by liquid scintillation spectrophotometry (3 mL scintillation cocktail). Assays were performed in triplicate. IC_{50} values were determined by fitting activity data to Equation (1) with nonlinear regression analysis using SigmaPlot v. 10.0 (Systat Software, San Jose, USA).

$$\text{fractional enzyme activity} = \frac{1}{1+\frac{[I]}{IC_{50}}} \quad (1)$$

PRMT1 (Npl3p substrate) inhibitory assay: A colorimetric assay was used as previously described[36] to determine inhibitory activities of test compounds against *h*PRMT1 using Npl3p as a nonhistone substrate. Briefly, 50 μL of a 10 μg μL^{-1} solution of GST-Npl3 protein in Tris-buffered saline (TBS) was added to each well of a clear 96-microtiter plate (Greiner Bio-one) with high binding affinity. After incubation overnight at 4 °C, the plate was rinsed twice with TBST (25 mM Tris (pH 7.5), 150 mM NaCl, 0.1% Tween 20), and once with 20 mM TBS (pH 8.0). The compounds were added (1 μL of 0.5 mM or 2.5 mM DMSO solutions) to the GST-Npl3-coated plates. After a 15 min incubation, 100 ng of *h*PRMT1 (0.03 μM) and 1 μL of SAM (0.1 mM stock, Sigma–Aldrich) were added to each well in a final volume of 50 μL of 20 mM Tris buffer (pH 8.0) and incubated at 30 °C for 1 h. The plate was washed with TBST and then blocked with 5% BSA in TBST buffer for 1.5 h at RT. Anti-Npl3 antibody 1E4 (1:1000)[68] was then added (50 μL) to each well and the plate was shaken for 2 h at RT. The wells were washed three times with TBST. Anti-mouse HRP IgG (GE Healthcare; 1:5000 dilution in TBST, 5% BSA) was then added as a secondary antibody to each well, and the mixture was incubated for 1 h at RT. The wells were again rinsed three times with TBST. The peroxidase substrate 2,2′-(hydrazine-1,2-diylidene)bis(3-ethyl-2,3-dihydrobenzo[*d*]thiazole-6-sulfonic acid) (ABTS, Roche) was added to each well (50 μL of 1 mg mL^{-1} solution), and the mixture was incubated for 30 min. The absorbance was measured at 405 nm with a plate reader (Bio-Rad).

PRMT1, PRMT3, PRMT4/CARM1, PRMT6 and SET7/9 in vitro methylation assays: In vitro methylation assays were described in detail previously.[36] Briefly, all methylation reactions were carried out in the presence of [^{3}H]SAM (0.42 μM, 79 Ci mmol^{-1}, stock solution in diluted HCl/EtOH 9:1, pH 2.0–2.5, GE Healthcare) and PBS (137 mM NaCl, 2.7 mM KCl, 4.3 mM Na_2HPO_4, 1.4 mM KH_2PO_4, pH 7.4). To determine the specificity of their inhibitory activities, test compounds were incubated with GST-PRMT1 (10×10^{-8} M) and histone H4 (all 1.5×10^{-6} M), GST-PRMT3 (9.0×10^{-8} M) and GAR (4.1×10^{-7} M), GST-PRMT4 (9.8×10^{-8} M) and histone H3 (all 1.1×10^{-6} M), GST-PRMT6 (9.7×10^{-8} M) and histone H3 and SET 7/9 (1.3×10^{-7} M) and histone H3. Histones were purchased from Roche. Substrates (0.5 μg, concentration range from 1.1×10^{-6} M to 4.06×10^{-7} M) were incubated with recombinant enzymes (0.2 μg, concentration range from 1.3×10^{-7} M to 10×10^{-8} M) in the presence of 0.5 μg [^{3}H]SAM (0.42 μM) and 50 μM of compound for 90 min at 30 °C in a final volume of 30 μL. Reactions were run on a 10% SDS-PAGE, transferred to a polyvinylidene fluoride (PVDF) membrane (Millipore), sprayed with Enhance™ (PerkinElmer) and exposed to film overnight. Band intensities were calculated using a Kodak Image Station 440 and 1D Image Analysis Software (Eastman Kodak Co.).

In vivo methylation assay: HeLa cells were labeled using a previously described in vivo methylation assay.[36,74] Briefly, HeLa cells were grown in 12-well plates and then transiently transfected with d2GFP-Npl3. For this GFP-Npl3 fusion construct, full-length Npl3 from pGEX-Npl3 was amplified by PCR primer 1 (5′-GTGGGATCCCACCATGTCTGAAGCTCAAGA-3′) and primer 2 (5′-AGAGGATCCAACCTGGTTGGTGATCTTTCACG-3′). The 5′ primer introduced a mammalian "Kozak" sequence (CACC) just upstream of the initiator sequence, ATG. The fragments were subcloned in pd2EGFP-N1 (Clontech, Palo Alto, USA) to generate an N-terminal fusion of Npl3. Three hours post-transfection, the cells were incubated with the indicated compounds (as DMSO solutions) for 24 h. The cells were lysed in a "mild" buffer (RIPA buffer; 150 mM NaCl, 5 mM EDTA, 1% Triton X-100, 10 mM Tris-HCl, pH 7.5) and Western analysis was performed with either the 1E4 antibody[68] or αGFP antibody (Clontech, Palo Alto, USA). The effects of the compounds on GFP-Npl3 methylation status were established with the methyl-specific antibody, 1E4. The αGFP antibody showed the protein levels of GFP-Npl3.

Molecular docking

All compounds were built, starting from ASCII text, using the standalone version of PRODRG,[75,76] in conjunction with the GROMACS suite.[77] Docking studies were performed on Autodock 3.0.5 using a grid spacing of 0.375 Å and $39\times50\times56$ number of points that embraced both the SAM and Arg binding sites. The grid was centered on the mass centre of the experimental bound SAM and Arg substrates. The GA-LS method was adopted using the default setting, except for the maximum number of energy evaluations which was increased from 250000 to 2500000. Autodock generated 100 possible binding conformations for each molecule that were clustered using a tolerance of 2.0 Å. The AutoDockTool (ADT) graphical interface[78] was used to prepare the enzyme PDBQS file. The protein atom charges as calculated during the complex minimization were retained for the docking calculations.

The SAM and *N*-acetyl,O-methyl-capped Arg PRODRG generated conformations were docked into the RmtA structure to assess the docking protocol. The SAM and Arg were docked back into their binding sites and the Xscore[71] selected conformations showed root mean square deviations (RMSD) of 0.60 and 1.47, respectively. The Autodock scoring function did not select conformations with lower RMSD values. The same trials were conducted using the DOCK program, however, attempts to dock these substrates back in to the RmtA binding site were unsuccessful, therefore we con-

tinued to use Autodock. ADT was used to analyze the docking results and Chimera 1.3 (build 2577)[79] was used to produce the images.

The outcomes of the docking experiments were supported by the application of our previous three-dimentional QSAR models,[40] yielding low errors of prediction (Supporting Information).

Glossary

AIB1, amplified in breast cancer-1; BL21, *Escherichia coli* B cells lacking the Lon protease; BSA, bovine serum albumin; CARM1, coactivator-associated arginine methyltransferase 1; CBP, CREB binding protein; CREB, *c*-AMP response-element binding; *a*DMA, asymmetrical dimethylarginine; *s*DMA, symmetrical dimethylarginine; FBXO11; F-box protein 11; GAR, glycine- and arginine-rich; GST, glutathione-*S*-transferase; HKMT, histone lysine methyltransferase; *hn*RNP, heterogeneous nuclear ribonucleoprotein; HRP, horseradish peroxidase; IPTG, isopropyl-β-D-1-thiogalactopyranoside; LB, lysogeny broth; MMA, monomethylarginine; NF-κB, nuclear factor κB; Npl3, nuclear shuttling protein; p300, E1A binding protein 300 kDa; PBS, phosphate buffer saline; PRMT, protein arginine methyltransferase; PVDF, polyvinylidene fluoride; RmtA, fungal arginine methyltransferase A; SAM, *S*-adenosyl methionine; SDS-PAGE, sodium dodecyl sulfatepolyacrylamide gel electrophoresis; SET, Su(var.) 3–9, enhancer-of-zeste and trithorax; TBS, Tris-buffered saline; TBST, Tris-buffered saline Tween-20; TCA, trichloroacetic acid.

Acknowledgements

Many thanks to Professors Gabriele Cruciani and Sergio Clementi (Molecular Discovery and MIA srl) for the use of the GOLPE program in their chemometric laboratory (University of Perugia, Italy) and for providing the GRID program. This work was partially supported by grants from Regione Campania 2003, LR 5/02 (G.S.), Ministero dell'Università e della Ricerca Scientifica e Tecnologica -PRIN 2007, (G.S.), Università di Salerno (G.S.), Ministero dell'Università e della Ricerca Scientifica e Tecnologica -PRIN (A. M.), RETI FIRB, (A. M.), Fondazione Roma (A. M.) and The Welch Foundation Grant G-1495 (M.T.B.).

Keywords: enzymes · epigenetics · histone methylation · inhibitors · transferases

[1] B. D. Strahl, C. D. Allis, *Nature* **2000**, *403*, 41–45.
[2] A. Shilatifard, *Annu. Rev. Biochem.* **2006**, *75*, 243–269.
[3] H. Li, S. Park, B. Kilburn, M. A. Jelinek, A. Henschen-Edman, D. W. Aswad, M. R. Stallcup, I. A. Laird-Offringa, *J. Biol. Chem.* **2002**, *277*, 44623–44630.
[4] M. T. Bedford, S. Richard, *Mol. Cell* **2005**, *18*, 263–272.
[5] S. Pahlich, R. P. Zakaryan, H. Gehring, *Biochim. Biophys. Acta Proteins Proteomics* **2006**, *1764*, 1890–1903.
[6] C. D. Krause, Z.-H. Yang, Y.-S. Kim, J.-H. Lee, J. R. Cook, S. Pestka, *Pharmacol. Ther.* **2007**, *113*, 50–87.
[7] J. M. Aletta, J. C. Hu, M. R. El-Gewely, *Biotechnol. Annu. Rev.* **2008**, *14*, 203–224.
[8] Y. Zhang, D. Reinberg, *Genes Dev.* **2001**, *15*, 2343–2360.
[9] M. T. Bedford, *J. Cell Sci.* **2007**, *120*, 4243–4246.
[10] F. Bachand, *Eukaryotic Cell* **2007**, *6*, 889–898.
[11] F. Herrmann, M. Bossert, A. Schwander, E. Akgun, F. O. Fackelmayer, *J. Biol. Chem.* **2004**, *279*, 48774–48779.
[12] S. S. Koh, D. Chen, Y.-H. Lee, M. R. Stallcup, *J. Biol. Chem.* **2001**, *276*, 1089–1098.
[13] B. D. Strahl, S. D. Briggs, C. J. Brame, J. A. Caldwell, S. S. Koh, H. Ma, R. G. Cook, J. Shabanowitz, D. F. Hunt, M. R. Stallcup, C. D. Allis, *Curr. Biol.* **2001**, *11*, 996–1000.
[14] H. Wang, Z.-Q. Huang, L. Xia, Q. Feng, H. Erdjument-Bromage, B. D. Strahl, S. D. Briggs, C. D. Allis, J. Wong, P. Tempst, Y. Zhang, *Science* **2001**, *293*, 853–857.
[15] S. L. Anzick, J. Kononen, R. L. Walker, D. O. Azorsa, M. M. Tanner, X.-Y. Guan, G. Sauter, O.-P. Kallioniemi, J. M. Trent, P. S. Meltzer, *Science* **1997**, *277*, 965–968.
[16] J. Torchia, D. W. Rose, J. Inostroza, Y. Kamei, S. Westin, C. K. Glass, M. G. Rosenfeld, *Nature* **1997**, *387*, 677–684.
[17] S.-K. Lee, S. L. Anzick, J.-E. Choi, L. Bubendorf, X.-Y. Guan, Y.-K. Jung, O. P. Kallioniemi, J. Kononen, J. M. Trent, D. Azorsa, B.-H. Jhun, J. H. Cheong, Y. C. Lee, P. S. Meltzer, J. W. Lee, *J. Biol. Chem.* **1999**, *274*, 34283–34293.
[18] Y. Zhu, C. Qi, S. Jain, M. M. Le Beau, R. Espinosa, G. B. Atkins, M. A. Lazar, A. V. Yeldandi, M. S. Rao, J. K. Reddy, *Proc. Natl. Acad. Sci. USA* **1999**, *96*, 10848–10853.
[19] H. Hong, C. Kao, M.-H. Jeng, J. N. Eble, M. O. Koch, T. A. Gardner, S. Zhang, L. Li, C.-X. Pan, Z. Hu, G. T. MacLennan, L. Cheng, *Cancer* **2004**, *101*, 83–89.
[20] S. Majumder, Y. Liu, O. H. Ford III, J. L. Mohler, Y. E. Whang, *Prostate* **2006**, *66*, 1292–1301.
[21] R. H. Böger, K. Sydow, J. Borlak, T. Thum, H. Lenzen, B. Schubert, D. Tsikas, S. M. Bode-Böger, *Circ. Res.* **2000**, *87*, 99–105.
[22] C. T. L. Tran, J. M. Leiper, P. Vallance, *Atheroscler. Suppl.* **2003**, *4*, 33–40.
[23] P. Vallance, J. Leiper, *Arterioscler. Thromb. Vasc. Biol.* **2004**, *24*, 1023–1030.
[24] J. Leiper, J. Murray-Rust, N. McDonald, P. Vallance, *Proc. Natl. Acad. Sci. USA* **2002**, *99*, 13527–13532.
[25] A. Leone, S. Moncada, P. Vallance, A. Calver, J. Collier, *Lancet* **1992**, *339*, 572–575.
[26] J. Leiper, M. Nandi, B. Torondel, J. Murray-Rust, M. Malaki, B. O'Hara, S. Rossiter, S. Anthony, M. Madhani, D. Selwood, C. Smith, B. Wojciak-Stothard, A. Rudiger, R. Stidwill, N. Q. McDonald, P. Vallance, *Nat. Med.* **2007**, *13*, 198–203.
[27] X. Chen, F. Niroomand, Z. Liu, A. Zankl, H. A. Katus, L. Jahn, C. P. Tiefenbacher, *Basic Res. Cardiol.* **2006**, *101*, 346–353.
[28] D. Cheng, J. Côté, S. Shaaban, M. T. Bedford, *Mol. Cell* **2007**, *25*, 71–83.
[29] J. Lee, M. T. Bedford, *EMBO Rep.* **2002**, *3*, 268–273.
[30] T. Fujiwara, Y. Mori, D. L. Chu, Y. Koyama, S. Miyata, H. Tanaka, K. Yachi, T. Kubo, H. Yoshikawa, M. Tohyama, *Mol. Cell. Biol.* **2006**, *26*, 2273–2285.
[31] P. O. Hassa, M. Covic, M. T. Bedford, M. O. Hottiger, *J. Mol. Biol.* **2008**, *377*, 668–678.
[32] N. Troffer-Charlier, V. Cura, P. Hassenboehler, D. Moras, J. Cavarelli, *EMBO J.* **2007**, *26*, 4391–4401.
[33] X. Zhang, X. Cheng, *Structure* **2003**, *11*, 509–520.
[34] X. Zhang, L. Zhou, X. Cheng, *EMBO J.* **2000**, *19*, 3509–3519.
[35] O. Obianyo, T. C. Osborne, P. R. Thompson, *Biochemistry* **2008**, *47*, 10420–10427.
[36] D. Cheng, N. Yadav, R. W. King, M. S. Swanson, E. J. Weinstein, M. T. Bedford, *J. Biol. Chem.* **2004**, *279*, 23892–23899.
[37] A. Mai, D. Cheng, M. T. Bedford, S. Valente, A. Nebbioso, A. Perrone, G. Brosch, G. Sbardella, F. De Bellis, M. Miceli, L. Altucci, *J. Med. Chem.* **2008**, *51*, 2279–2290.
[38] A. Mai, S. Valente, D. Cheng, A. Perrone, R. Ragno, S. Simeoni, G. Sbardella, G. Brosch, A. Nebbioso, M. Conte, L. Altucci, M. T. Bedford, *ChemMedChem* **2007**, *2*, 987–991.
[39] A. V. Purandare, Z. Chen, T. Huynh, S. Pang, J. Geng, W. Vaccaro, M. A. Poss, J. Oconnell, K. Nowak, L. Jayaraman, *Bioorg. Med. Chem. Lett.* **2008**, *18*, 4438–4441.
[40] R. Ragno, S. Simeoni, S. Castellano, C. Vicidomini, A. Mai, A. Caroli, A. Tramontano, C. Bonaccini, P. Trojer, I. Bauer, G. Brosch, G. Sbardella, *J. Med. Chem.* **2007**, *50*, 1241–1253.
[41] A. Spannhoff, R. Heinke, I. Bauer, P. Trojer, E. Metzger, R. Gust, R. Schule, G. Brosch, W. Sippl, M. Jung, *J. Med. Chem.* **2007**, *50*, 2319–2325.
[42] A. Spannhoff, R. Machmur, R. Heinke, P. Trojer, I. Bauer, G. Brosch, R. Schüle, W. Hanefeld, W. Sippl, M. Jung, *Bioorg. Med. Chem. Lett.* **2007**, *17*, 4150–4153.

[43] T. Osborne, R. L. Weller Roska, S. R. Rajski, P. R. Thompson, *J. Am. Chem. Soc.* **2008**, *130*, 4574 – 4575.
[44] M. Allan, S. Manku, E. Therrien, N. Nguyen, S. Styhler, M.-F. Robert, A.-C. Goulet, A. J. Petschner, G. Rahil, A. R. MacLeod, R. Déziel, J. M. Besterman, H. Nguyen, A. Wahhab, *Bioorg. Med. Chem. Lett.* **2009**, *19*, 1218 – 1223.
[45] R. Heinke, A. Spannhoff, R. Meier, P. Trojer, I. Bauer, M. Jung, W. Sippl, *ChemMedChem* **2009**, *4*, 69 – 77.
[46] H. Wan, T. Huynh, S. Pang, J. Geng, W. Vaccaro, M. A. Poss, G. L. Trainor, M. V. Lorenzi, M. Gottardis, L. Jayaraman, A. V. Purandare, *Bioorg. Med. Chem. Lett.* **2009**, *19*, 5063 – 5066.
[47] Recently, Thompson and co-workers reported the preparation of a potent and selective bisubstrate inhibitor by the PRMT1-catalyzed reaction between peptide AcH4-21 and a SAM congener, 5′-(diaminobutyric acid)-*N*-iodoethyl-5′-deoxyadenosine ammonium hydrochloride (AAI).[43] Such a peptide-based bisubstrate analogue is unlikely to possess drug-like properties, but it could be a very useful tool for "chemical genetics" studies of PRMT function in vitro and in vivo.
[48] S. Massa, A. Mai, G. Sbardella, M. Esposito, R. Ragno, P. Loidl, G. Brosch, *J. Med. Chem.* **2001**, *44*, 2069 – 2072.
[49] A. Mai, S. Massa, R. Ragno, M. Esposito, G. Sbardella, G. Nocca, R. Scatena, F. Jesacher, P. Loidl, G. Brosch, *J. Med. Chem.* **2002**, *45*, 1778 – 1784.
[50] P. Ornaghi, D. Rotili, G. Sbardella, A. Mai, P. Filetici, *Biochem. Pharmacol.* **2005**, *70*, 911 – 917.
[51] S. Bartolini, A. Mai, M. Artico, N. Paesano, D. Rotili, C. Spadafora, G. Sbardella, *J. Med. Chem.* **2005**, *48*, 6776 – 6778.
[52] G. Sbardella, S. Bartolini, S. Castellano, M. Artico, N. Paesano, D. Rotili, C. Spadafora, A. Mai, *ChemMedChem* **2006**, *1*, 1073 – 1080.
[53] A. Mai, D. Rotili, D. Tarantino, P. Ornaghi, F. Tosi, C. Vicidomini, G. Sbardella, A. Nebbioso, M. Miceli, L. Altucci, P. Filetici, *J. Med. Chem.* **2006**, *49*, 6897 – 6907.
[54] G. Sbardella, S. Castellano, C. Vicidomini, D. Rotili, A. Nebbioso, M. Miceli, L. Altucci, A. Mai, *Bioorg. Med. Chem. Lett.* **2008**, *18*, 2788 – 2792.
[55] S. Castellano, D. Kuck, M. Sala, E. Novellino, F. Lyko, G. Sbardella, *J. Med. Chem.* **2008**, *51*, 2321 – 2325.
[56] R. Ragno, A. Mai, S. Simeoni, A. Caroli, S. Valente, A. Perrone, S. Castellano, G. Sbardella, *Small-Molecule Inhibitors of Histone Arginine Methyltransferases: Updated Structure-Based 3-D QSAR Models with Improved Robustness and Predictive Ability*; Frontiers in CNS and Oncology Medicinal Chemistry conference, ACS–EFMC, Siena (Italy), October 7 – 9, **2007**, pp. COMC-010.
[57] Color versions of Figures 2, 5–8 are available in the Supporting Information.
[58] Y.-L. Zhang, Y.-F. Keng, Y. Zhao, L. Wu, Z.-Y. Zhang, *J. Biol. Chem.* **1998**, *273*, 12281 – 12287.
[59] R. P. McGeary, A. J. Bennett, Q. B. Tran, K. L. Cosgrove, B. P. Ross, *Mini-Rev. Med. Chem.* **2008**, *8*, 1384 – 1394.
[60] S. Castellano, C. Milite, P. Campiglia, G. Sbardella, *Tetrahedron Lett.* **2007**, *48*, 4653 – 4655.
[61] S. Doulut, I. Dubuc, M. Rodriguez, F. Vecchini, H. Fulcrand, H. Barelli, F. Checler, E. Bourdel, A. Aumelas, *J. Med. Chem.* **1993**, *36*, 1369 – 1379.
[62] All attempts to obtain the pure acid **5b** from the corresponding ester **5a** failed.
[63] These experimental conditions lead to the partial hydrolysis of the 4-acetoxy to a 4-hydroxy group. As this did not influence the reaction, the crude mixture of the trichloroacetamides **18** was directly used in the following step.
[64] P. Trojer, M. Dangl, I. Bauer, S. Graessle, P. Loidl, G. Brosch, *Biochemistry* **2004**, *43*, 10834 – 10843.
[65] A. E. McBride, J. T. Cook, E. A. Stemmler, K. L. Rutledge, K. A. McGrath, J. A. Rubens, *J. Biol. Chem.* **2005**, *280*, 30888 – 30898.
[66] R. L. Bartel, R. T. Borchardt, *Mol. Pharmacol.* **1984**, *25*, 418 – 424.
[67] C. Schwerk, K. Schulze-Osthoff, *Oncogene* **2005**, *24*, 7002 – 7011.
[68] C. W. Siebel, C. Guthrie, *Proc. Natl. Acad. Sci. USA* **1996**, *93*, 13641 – 13646.
[69] In the case of CARM1/H3 incubations with tested compounds, we were not able to get strong bands on the fluorograph film and therefore we did not scan it.
[70] D. S. Goodsell, G. M. Morris, A. J. Olson, *J. Mol. Recognit.* **1996**, *9*, 1 – 5.
[71] R. Wang, L. Lai, S. Wang, *J. Comput.-Aided Mol. Des.* **2002**, *16*, 11 – 26.
[72] G. Bertani, *J. Bacteriol.* **2004**, *186*, 595 – 600.
[73] A. Frankel, N. Yadav, J. Lee, T. L. Branscombe, S. Clarke, M. T. Bedford, *J. Biol. Chem.* **2002**, *277*, 3537 – 3543.
[74] Q. Liu, G. Dreyfuss, *Mol. Cell. Biol.* **1995**, *15*, 2800 – 2808.
[75] A. W. Schüttelkopf, D. M. F. van Aalten, *Acta Crystallogr., Sect. D: Biol. Crystallogr.* **2004**, *60*, 1355 – 1363.
[76] PRODRG2 is freely available for academic research purposes at: http://davapc1.bioch.dundee.ac.uk/prodrg/index.html.
[77] D. Van Der Spoel, E. Lindahl, B. Hess, G. Groenhof, A. E. Mark, H. J. C. Berendsen, *J. Comput. Chem.* **2005**, *26*, 1701 – 1718.
[78] A. Gillet, M. Sanner, D. Stoffler, A. Olson, *Structure* **2005**, *13*, 483 – 491.
[79] E. F. Pettersen, T. D. Goddard, C. C. Huang, G. S. Couch, D. M. Greenblatt, E. C. Meng, T. E. Ferrin, *J. Comput. Chem.* **2004**, *25*, 1605 – 1612.

Received: November 7, 2009
Revised: December 11, 2009
Published online on January 20, 2010

